Study of Giant resonances in Exotic Nuclei by Means of Reactions in Inverse Kinematics

Muhsin N. Harakeh

University of Groningen, the Netherlands

3rd NUclear physics School for Young Scientists (NUSYS)

Fudan University, Shanghai

6-12 August 2023

Giant Resonances in hydrodynamic models

Coherent vibrations of nucleonic fluids (p & n; ↑ & ↓) in a nucleus

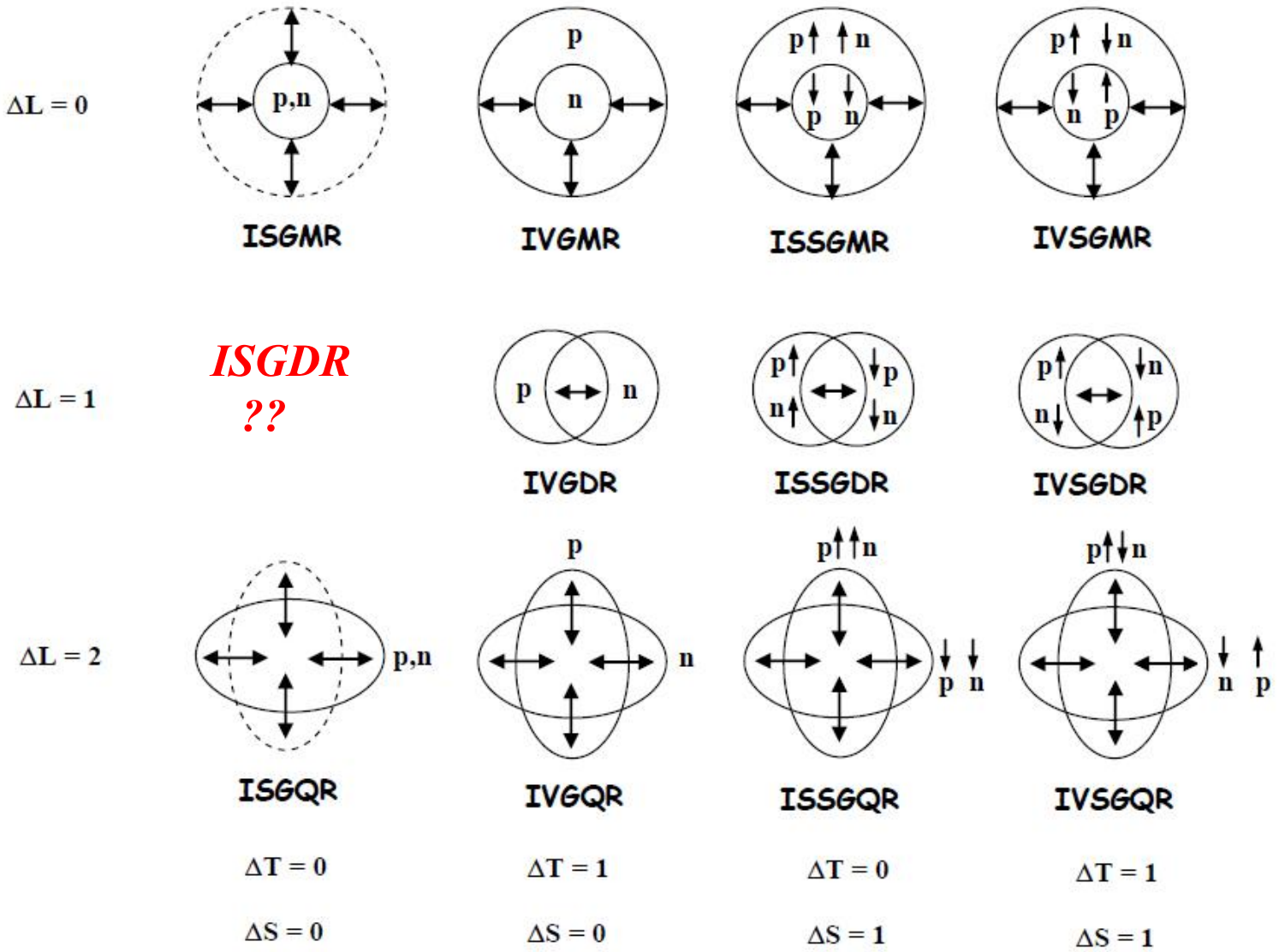

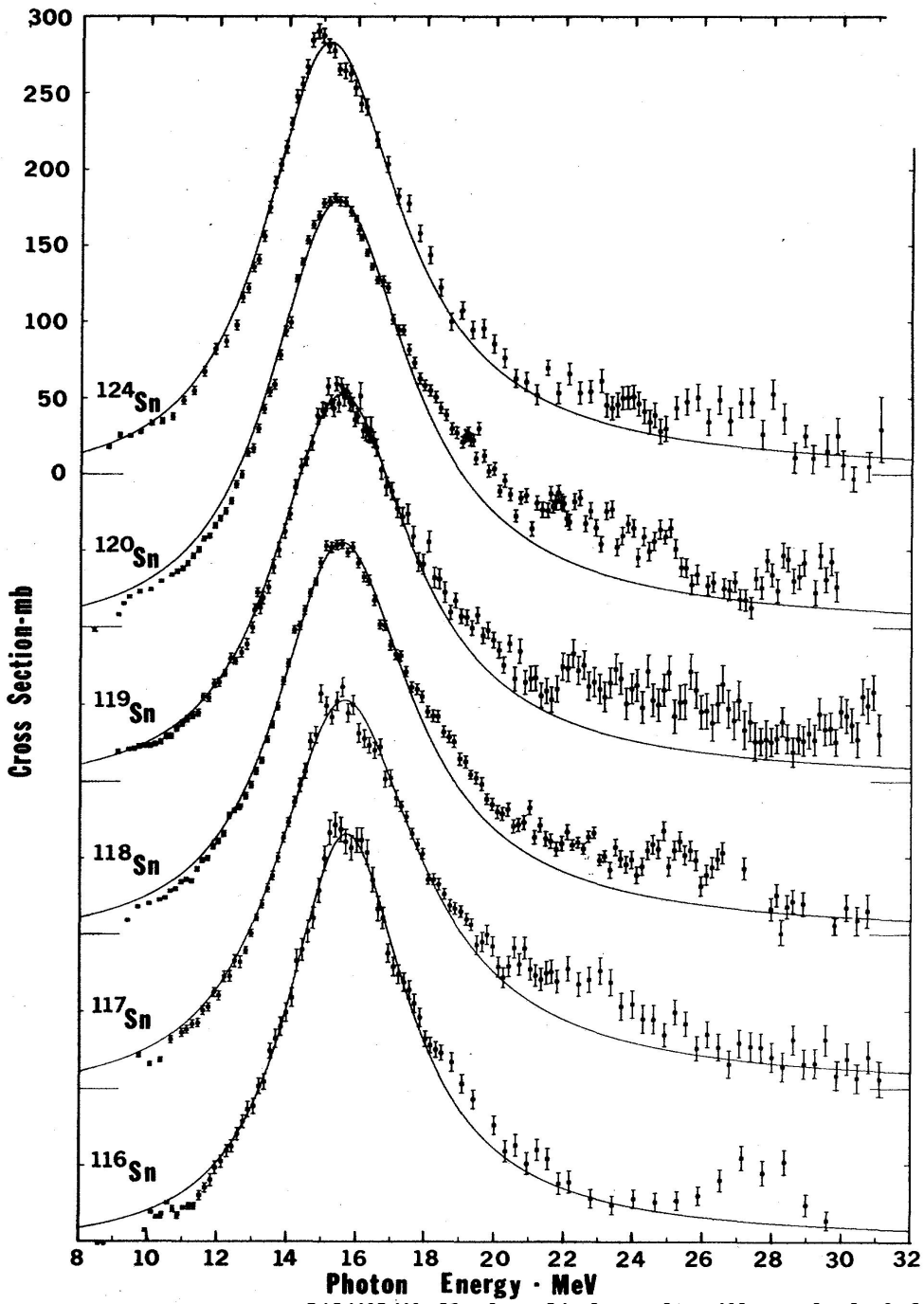

Measurement of the giant dipole resonance with mono-energetic photons

B.L. Berman and S.C. Fultz
Rev. Mod. Phys. 47 (1975) 713

Nucleus	Centroid (MeV)	Width (MeV)
^{116}Sn	15.68	4.19
^{117}Sn	15.66	5.02
^{118}Sn	15.59	4.77
^{119}Sn	15.53	4.81
^{120}Sn	15.40	4.89
^{124}Sn	15.19	4.81

Photo-neutron cross section in deformed nuclei:

Deformed Nucleus

$$R(\theta,\phi)=R_0(1+\beta_2 Y_{20}(\theta,\phi))$$

β_2 (^{150}Nd) = 0.285(3)

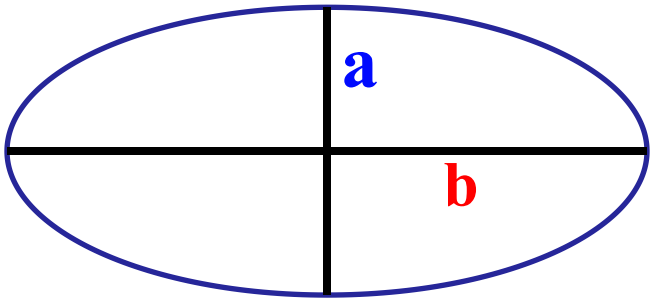

Excitation energies:

$E_2/E_1 = 0.911\eta + 0.089$

Where $\eta = b/a$

$S_1/S_2 = 1/2$

B. L. Berman and S. C. Fultz,
Rev. Mod. Phys. 47, 713 (1975)

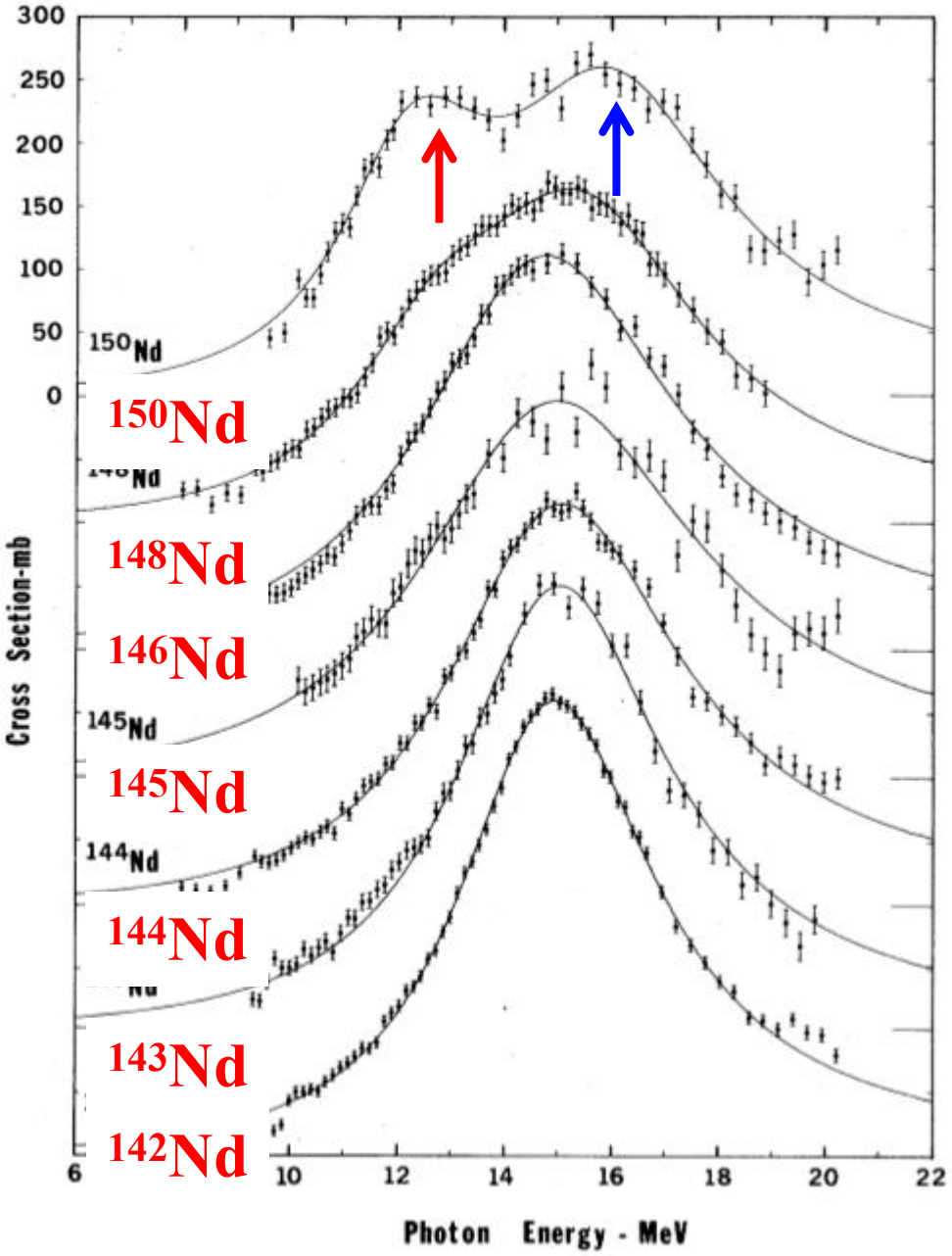

Experimental Tool: Electromagnetic excitation at high energies

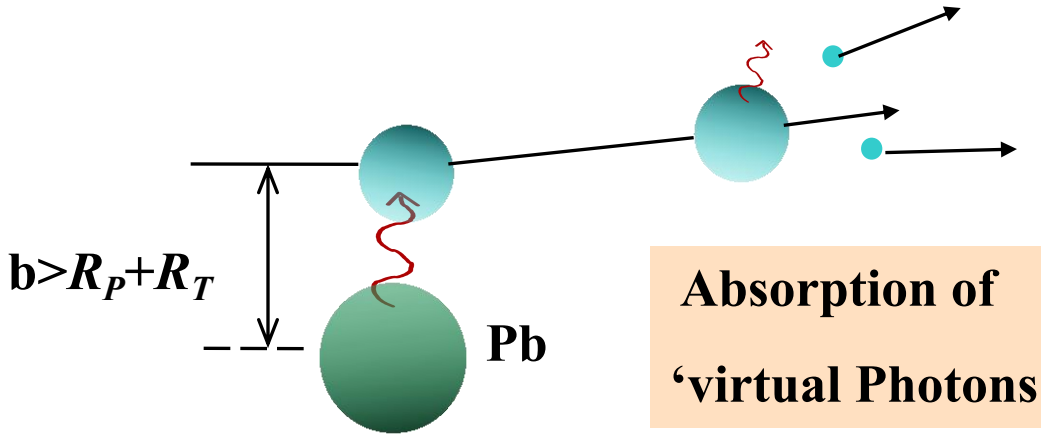

Absorption of 'virtual Photons'

Semi-classical theory:

$$d\sigma_{e.m.} / dE = N_\gamma(E)\, s_\gamma(E)$$

$$\sigma_{e.m.} \sim Z^2$$

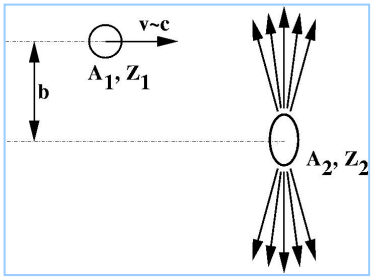

adiabatic cut-off:

$$E_{\max} = \frac{\hbar}{\tau} = \frac{\hbar c \gamma \beta}{b}$$

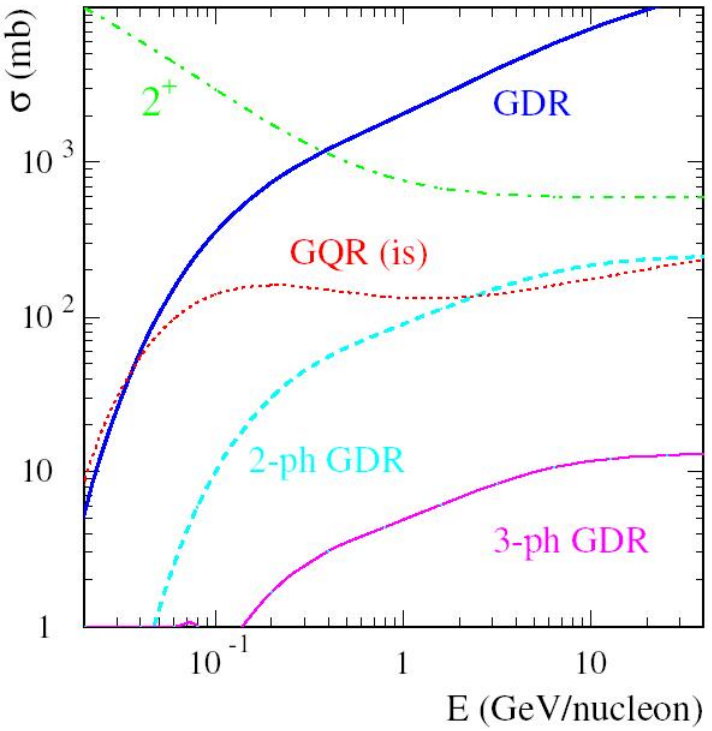

High velocities v/c ≈ 0.6-0.9
⇒ High-frequency Fourier components
$E_{\gamma,max}$ ≈ 25 MeV (@ 1 GeV/u)

Determination of 'photon energy' (excitation energy) via a kinematically complete measurement of the momenta of all outgoing particles (invariant mass)

Experimental Scheme: The LAND reaction setup @GSI

Mixed beam

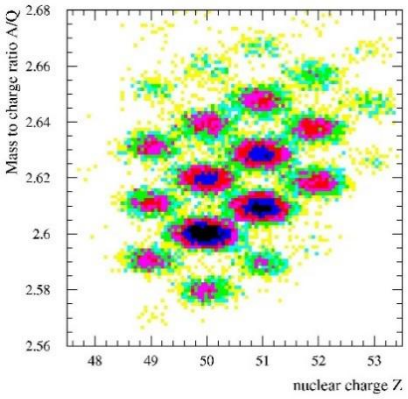

Charged fragments

ToF, ΔE

tracking → Bρ ~ A/Qβγ

LAND

Neutrons

ToF, x, y, z

~12 m

Photons

projectile tracking

ALADIN

large-acceptance dipole

Beam

Crystal Ball and Target

Excitation energy E* from kinematically complete measurement of all outgoing particles:

$$E^* = \left(\sqrt{\sum_i m_i^2 + \sum_{i \neq j} m_i m_j \gamma_i \gamma_j (1 - \beta_i \beta_j \cos\theta_{ij})} - m_{proj} \right) c^2 + E_\gamma$$

Dipole strength distributions in neutron-rich Sn isotopes

Electromagnetic-excitation cross section

Photo-neutron cross section

E(^{A}Sn) ~ 500 MeV/nucleon

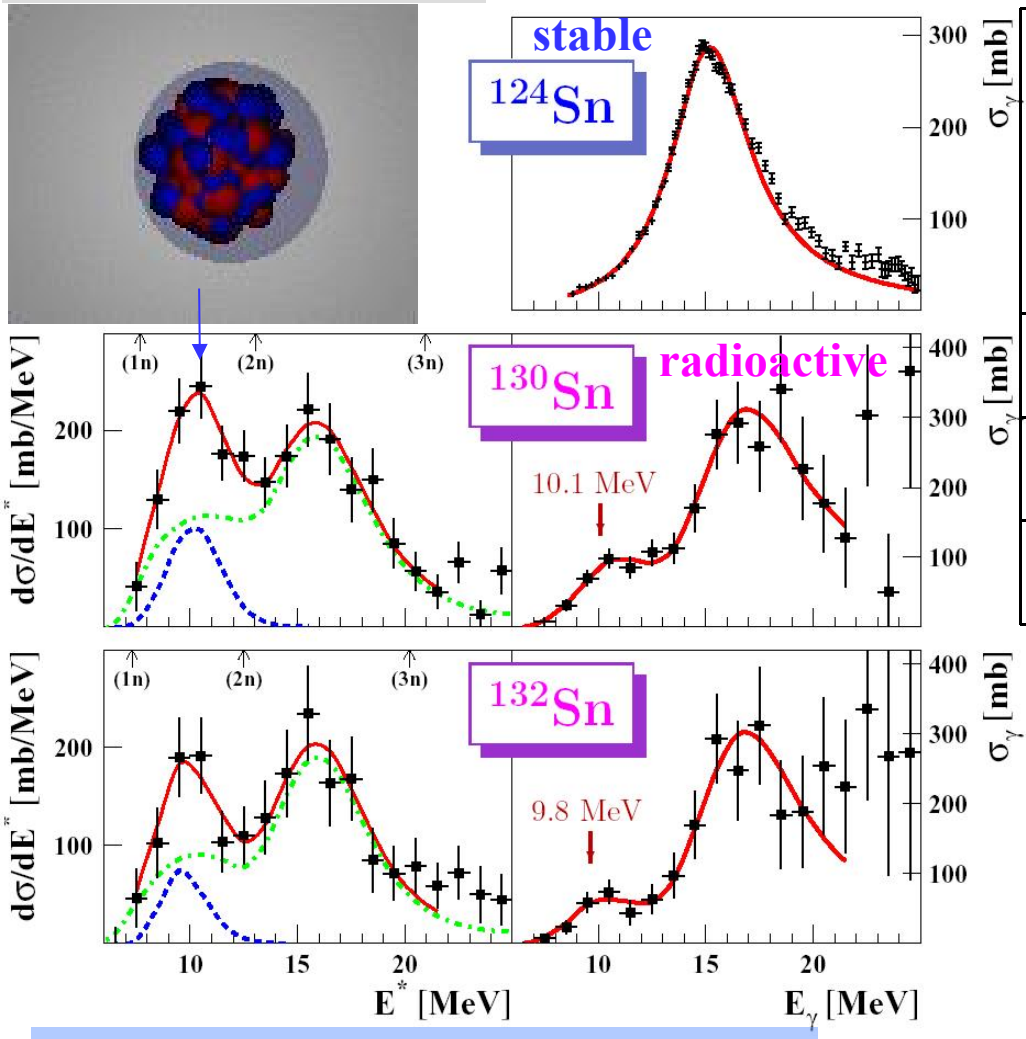

A	PDR		GDR		
	E_{centr} [MeV]	sum-rule fraction [%]	E_{centr} [MeV]	Γ [MeV]	sum-rule fraction [%]
^{124}Sn	-	-	15.3	4.8	116
^{130}Sn	10.1 (0.7)	7.0 (3.0)	15.9 (0.5)	4.8 (1.8)	145 (19)
^{132}Sn	9.8 (0.7)	4.0 (3.1)	16.1 (0.8)	4.7 (2.2)	125 (32)

Virtual photon spectra decrease as a function of virtual photon energy => correct for that!

PDR

- **located at 10 MeV**
- **exhausts a few % TRK sum rule**
- **in agreement with theory**

GDR

- **no deviation from systematics**

P. Adrich *et al.*, PRL 95 (2005) 132501

Dipole Strength Distribution of n-Rich Nuclei

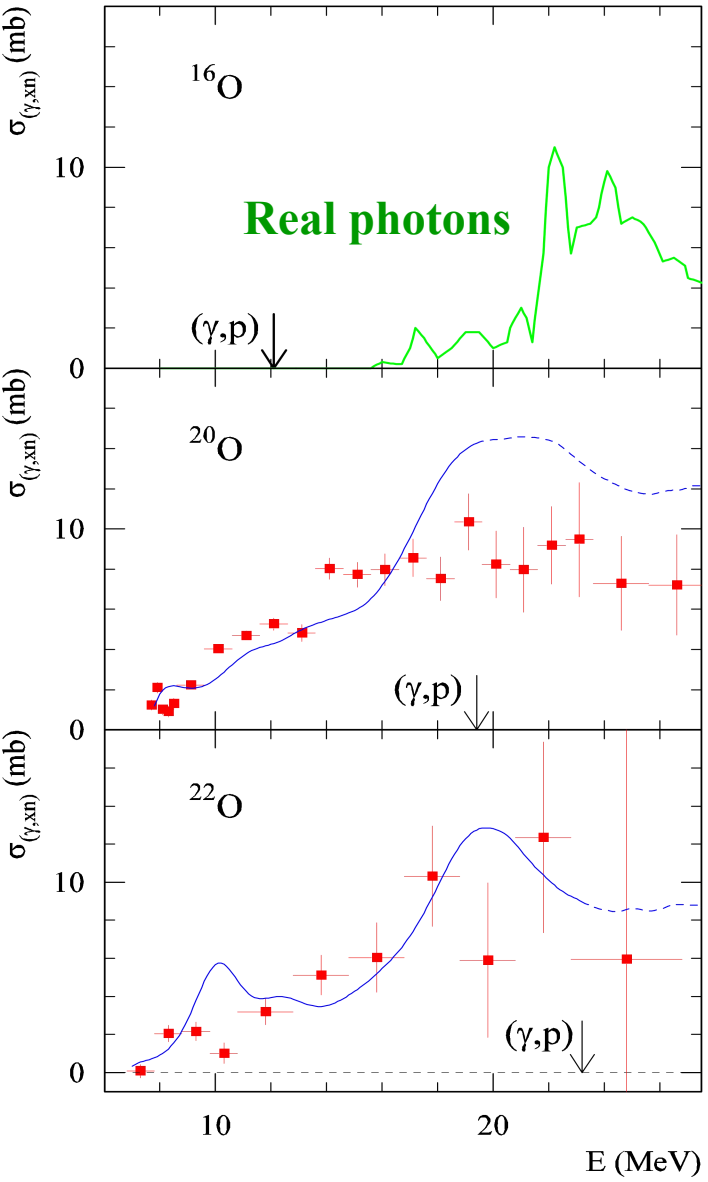

^{A}O (~ 500 MeV/u) + Pb → $^{A-x}$O + γ + *xn*

N-Z=0

⇒ Photo-neutron cross sections from virtual photons

N-Z=4

⇒ Low-lying dipole strength

⇒ Fragmentation of GDR strength

? Collective soft mode ?

N-Z=6

— Large-scale shell model calculation

H. Sagawa, T. Suzuki,

Phys. Rev. C 59 (1999) 3116

Data: LAND-FRS@GSI

A. Leistenschneider *et al.*, Phys. Rev. Lett. 86 (2001) 5442

Dipole strength distributions in ^{68}Ni

^{68}Ni incident energy 600 MeV/u

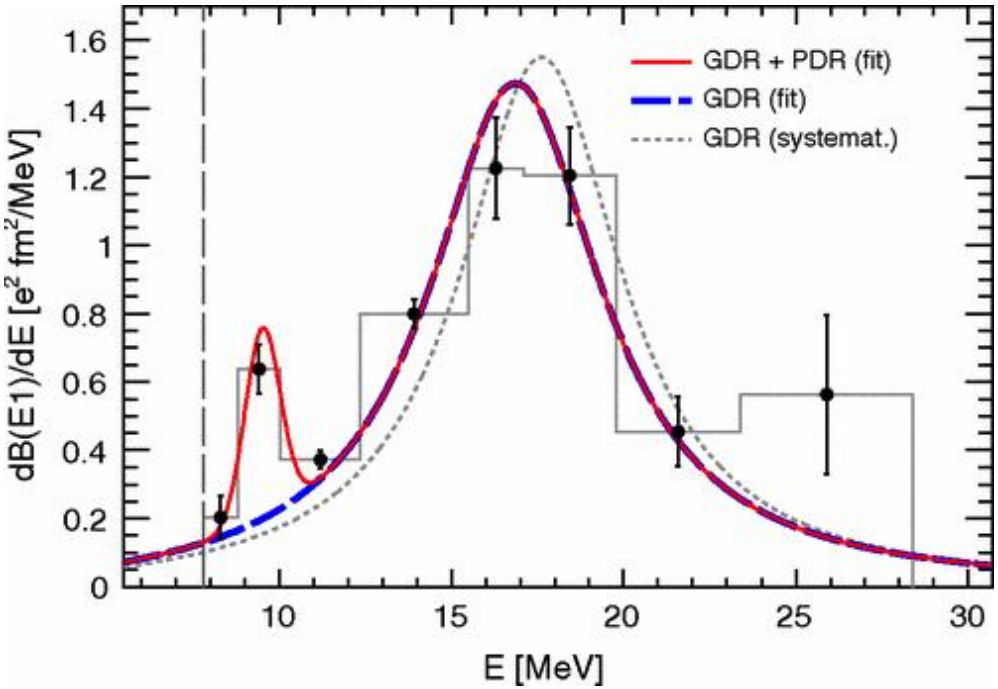

E1 strength distribution (histogram and black data points) with IVGDR+PDR fit function (solid red line). The IVGDR contribution (dashed blue line) and the IVGDR from systematics (dotted gray line) are shown for reference. The neutron threshold is indicated by the dashed vertical line at 7.792 MeV.

	E (MeV)	Γ (MeV)	%EWSR
IVGDR	17.1(2)	6.1(5)	98(7)
PDR	9.55(17)	0.51(13)	2.8(5)

D. Rossi *et al.*, Phys. Rev. Lett. 111 (2013) 242503

Distribution of isovector dipole strength for the three closed-(sub)shell nickel isotopes ^{56}Ni, ^{68}Ni, and ^{78}Ni calculated in HF-plus-RPA using the FSUGold interaction parameter set.

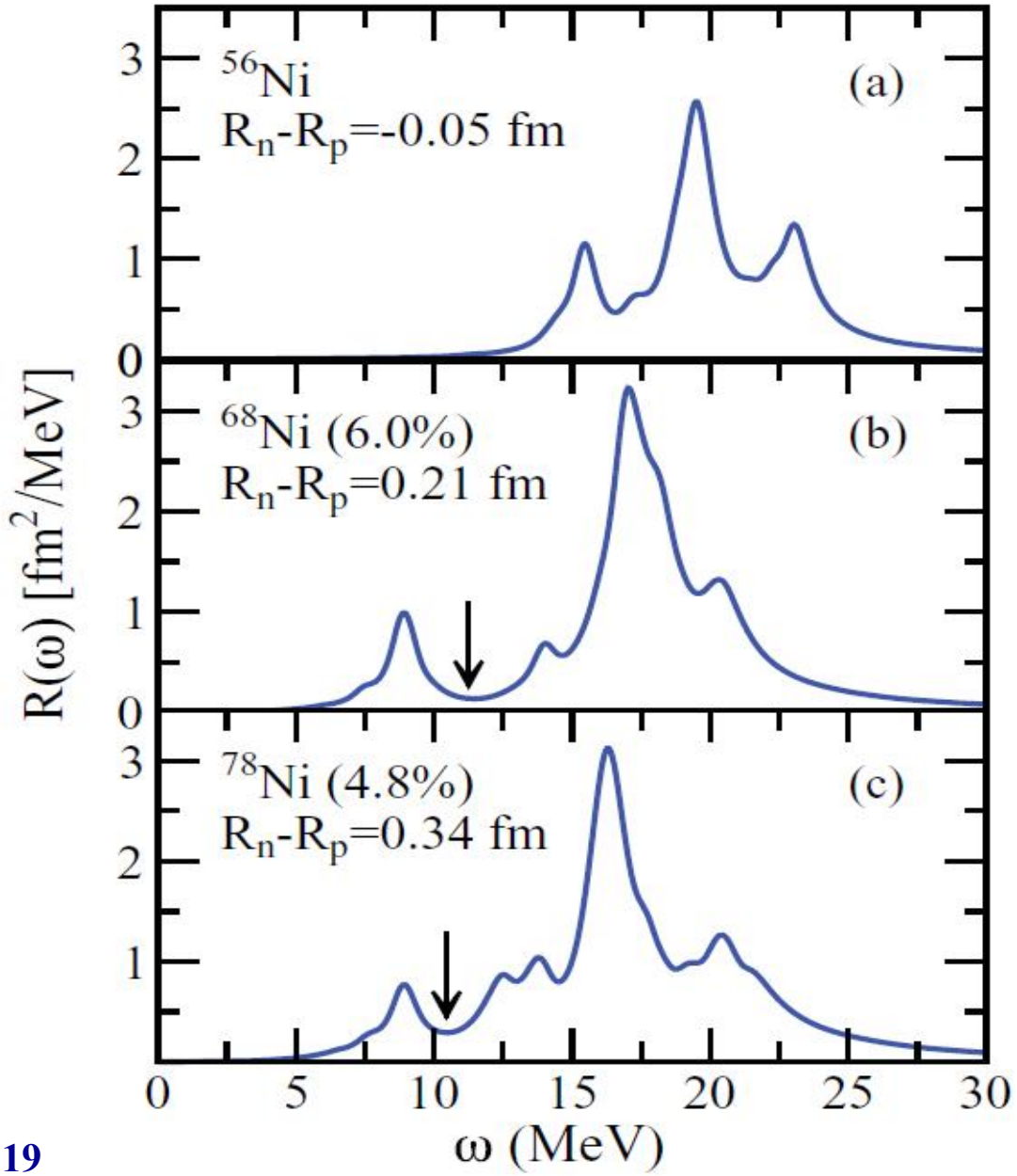

J. Piekarewicz, PRC 83 (2011) 034319

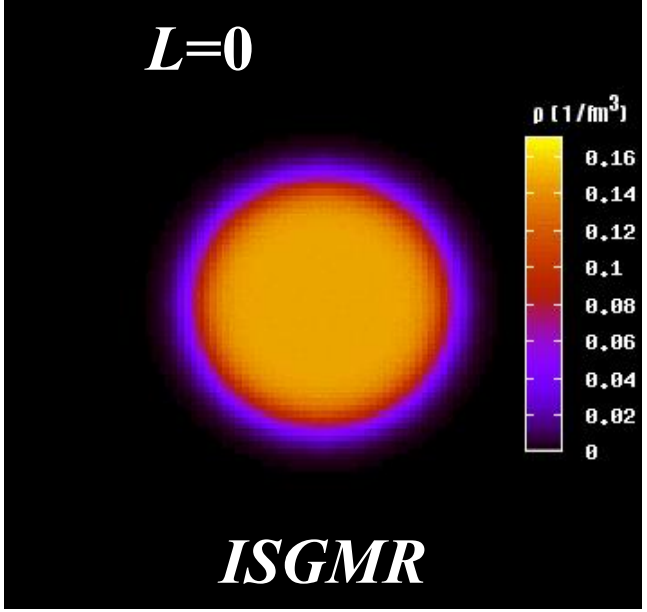

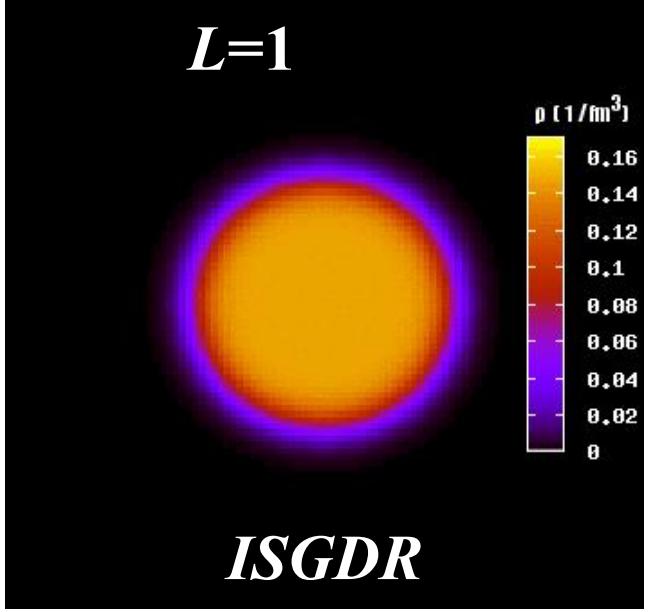

Macroscopic hydrodynamic description of L=0-3 isoscalar giant multipole resonances

ISGMR & ISGDR compression modes

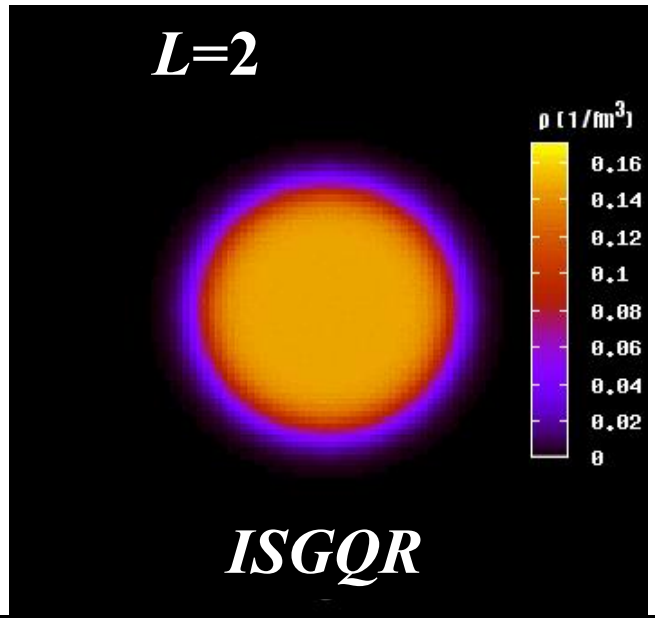

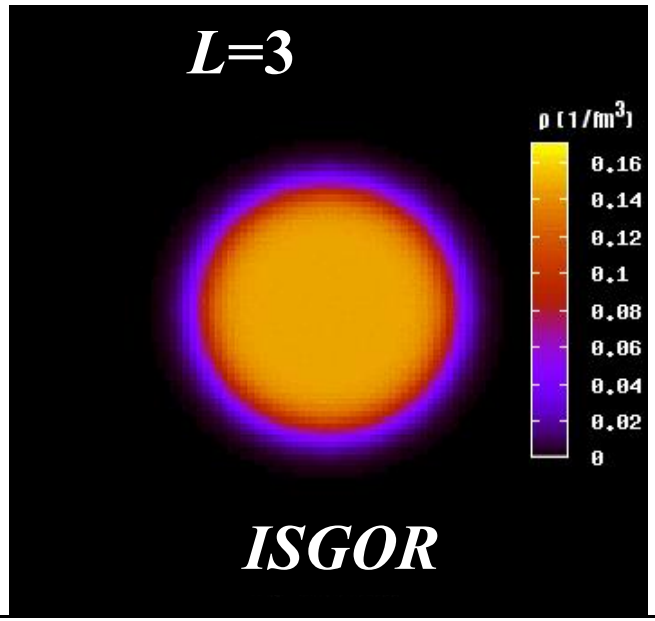

Drawing by Masatoshi Itoh

Compression Modes of Nuclei

Compression modes: ISGMR, ISGDR

In Constrained and Scaling Models:

$$E_{ISGMR} = \hbar\sqrt{\frac{K_A}{m\langle r^2\rangle}}$$

$$E_{ISGDR} = \hbar\sqrt{\frac{7}{3}\frac{K_A + \frac{27}{25}\varepsilon_F}{m\langle r^2\rangle}}$$

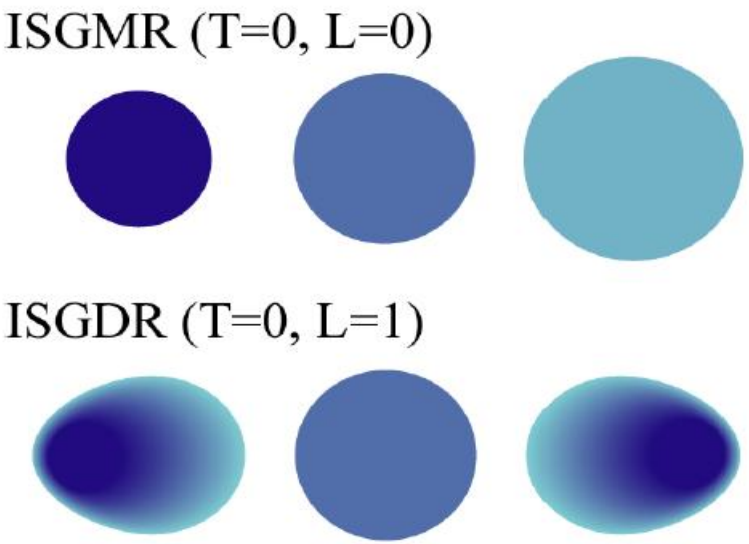

ε_F **is the Fermi energy and** K_A **is the nucleus incompressibility**

→ **ISGMR, ISGDR ⇒ Incompressibility, symmetry energy**

$$K_A = K_{vol} + K_{surf}A^{-1/3} + K_{sym}((N-Z)/A)^2 + K_{Coul}Z^2A^{-4/3}$$

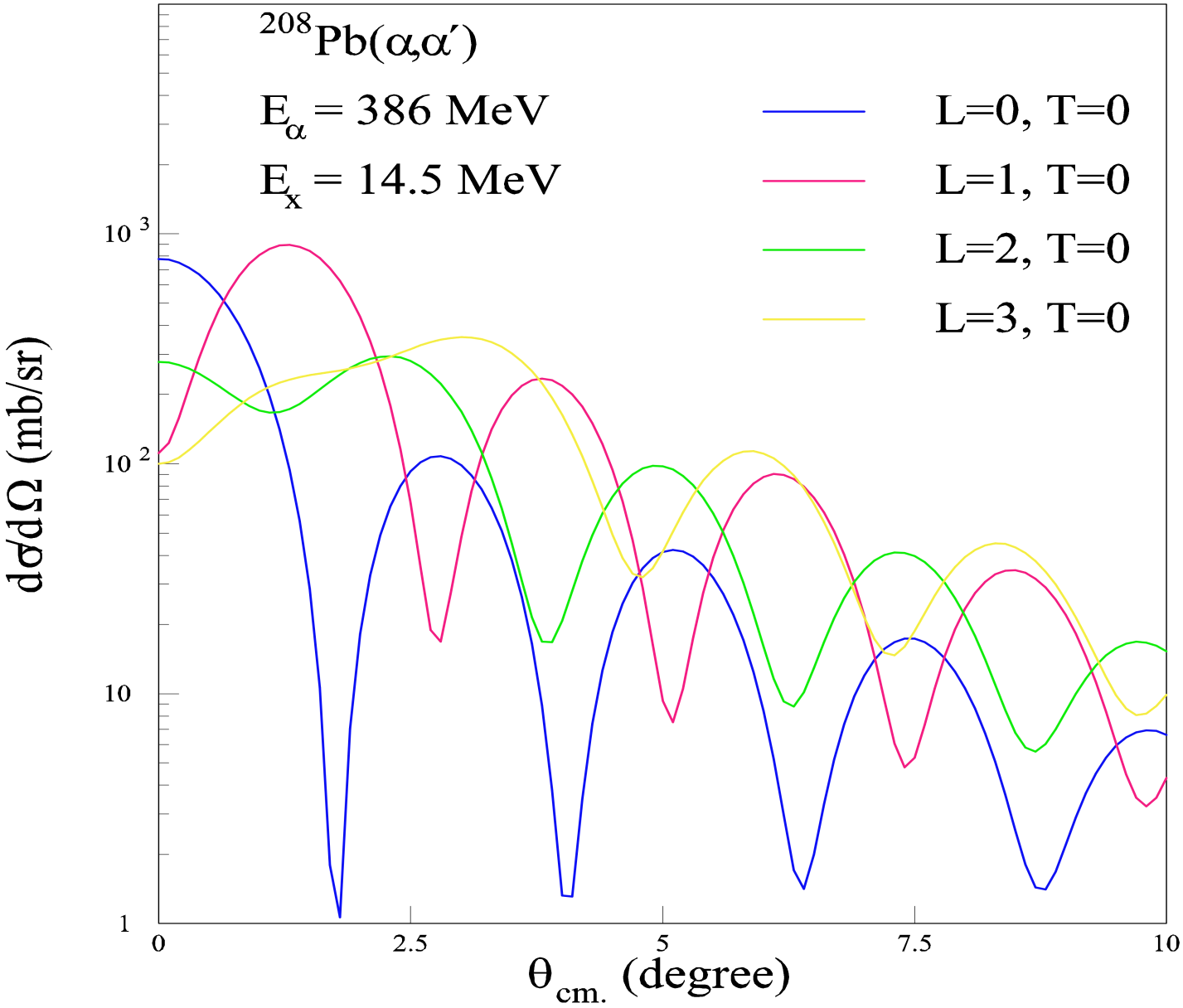

ISGMR, ISGDR

ISGQR, HEOR

100 % EWSR

At E_x= 14.5 MeV

Experiments at RCNP, Osaka University

- **(α,α′) reaction at ~ 400 MeV**
  - **High-resolution spectrometer “Grand Raiden”**

Uchida *et al.*,
Phys. Lett. B557 (2003) 12
Phys. Rev. C69 (2004) 051301

(α,α′) spectra at 386 MeV

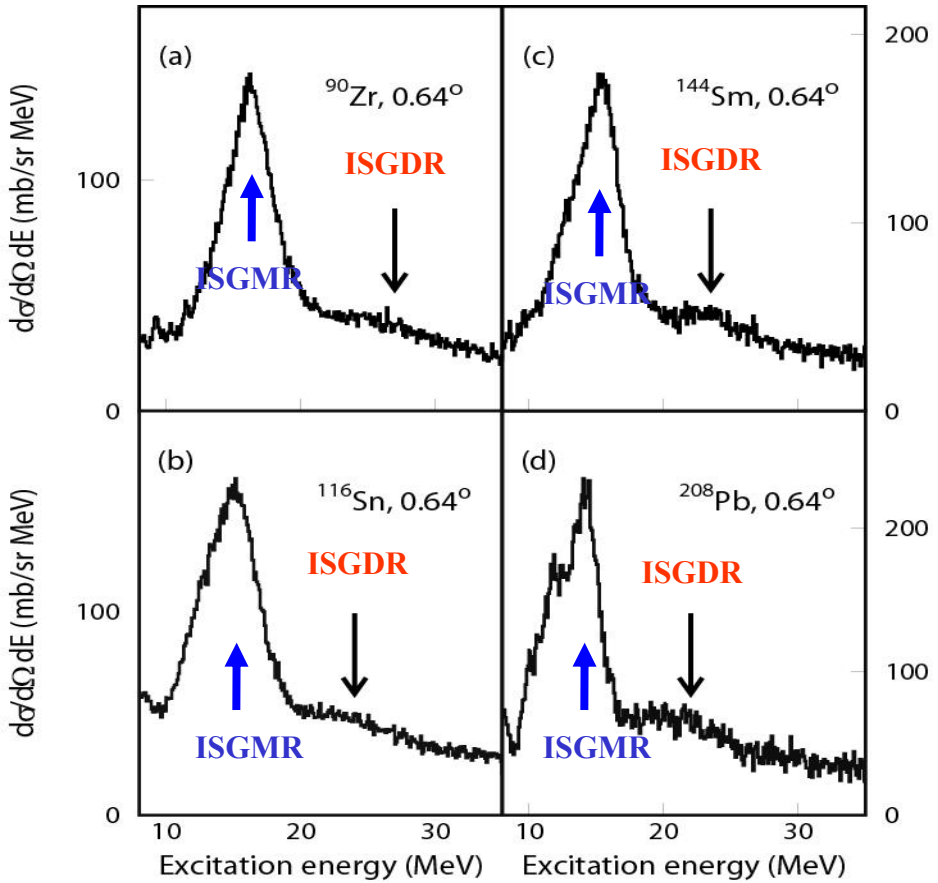

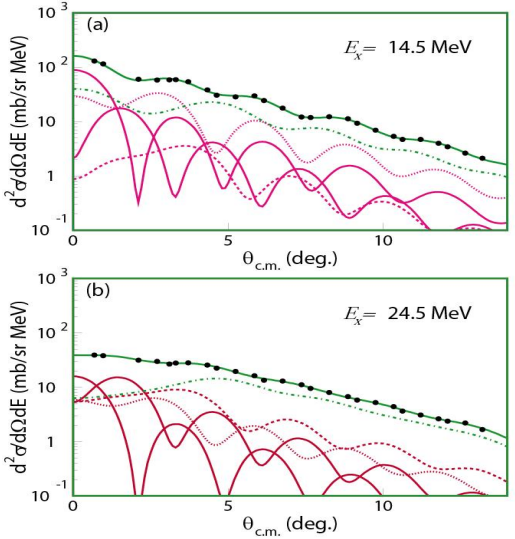

^{116}Sn

MDA results for *L=0* and *L=1*

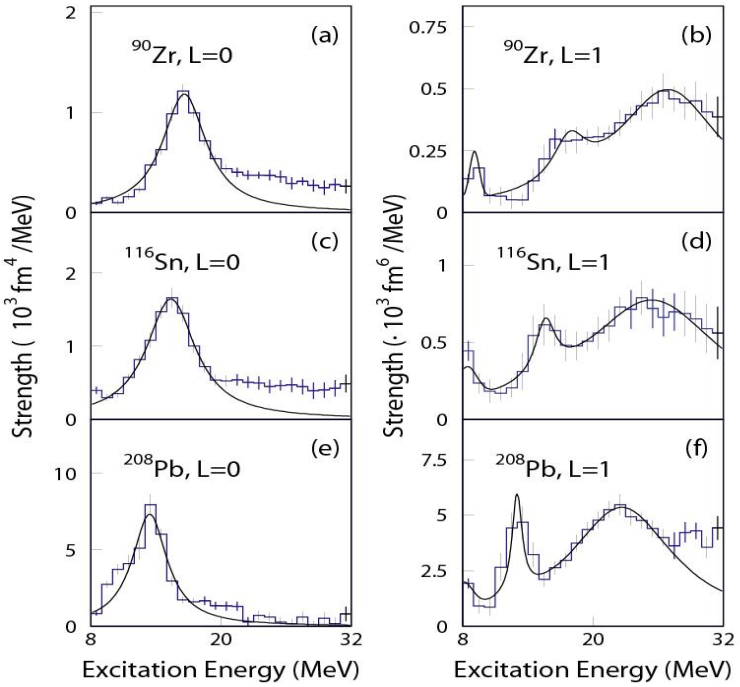

From GMR data on ^{208}Pb and ^{90}Zr,

$K_\infty = 240 \pm 10$ ($\pm$ 20) MeV

[See, *e.g.*, G. Colò *et al.*, Phys. Rev. C 70 (2004) 024307]

This number is consistent
with both ISGMR and ISGDR Data
and
with non-relativistic and relativistic calculations.

Z.Z. Li, Y.F. Niu, and G. Colò, Phys. Rev. Lett. accepted
QRPA+QPVC for ^{208}Pb, $^{112\text{-}124}$Sn and ^{48}Ca
K_∞ = 226 MeV and 229 MeV

$$K_A = K_{vol} + K_{surf}A^{-1/3} + K_{sym}((N-Z)/A)^2 + K_{coul}Z^2A^{-4/3}$$

$$K_A \sim K_{vol}(1 + cA^{-1/3}) + K_\tau((N - Z)/A)^2 + K_{Coul}Z^2A^{-4/3}$$

$$K_A - K_{Coul}Z^2A^{-4/3} \sim K_{vol}(1 + cA^{-1/3}) + K_\tau((N - Z)/A)^2$$

$$\sim \text{Constant} + K_\tau((N - Z)/A)^2$$

We use $K_{Coul} = -5.2$ MeV (from Sagawa)

$$(N - Z)/A$$

^{112}Sn – ^{124}Sn: 0.107 – 0.194

Isoscalar GMR strength distribution in Sn-isotopes obtained by Multipole Decomposition Analysis of singles spectra obtained in ^{A}Sn(α,α′) measurements at incident energy 400 MeV and angles from 0° to 9°

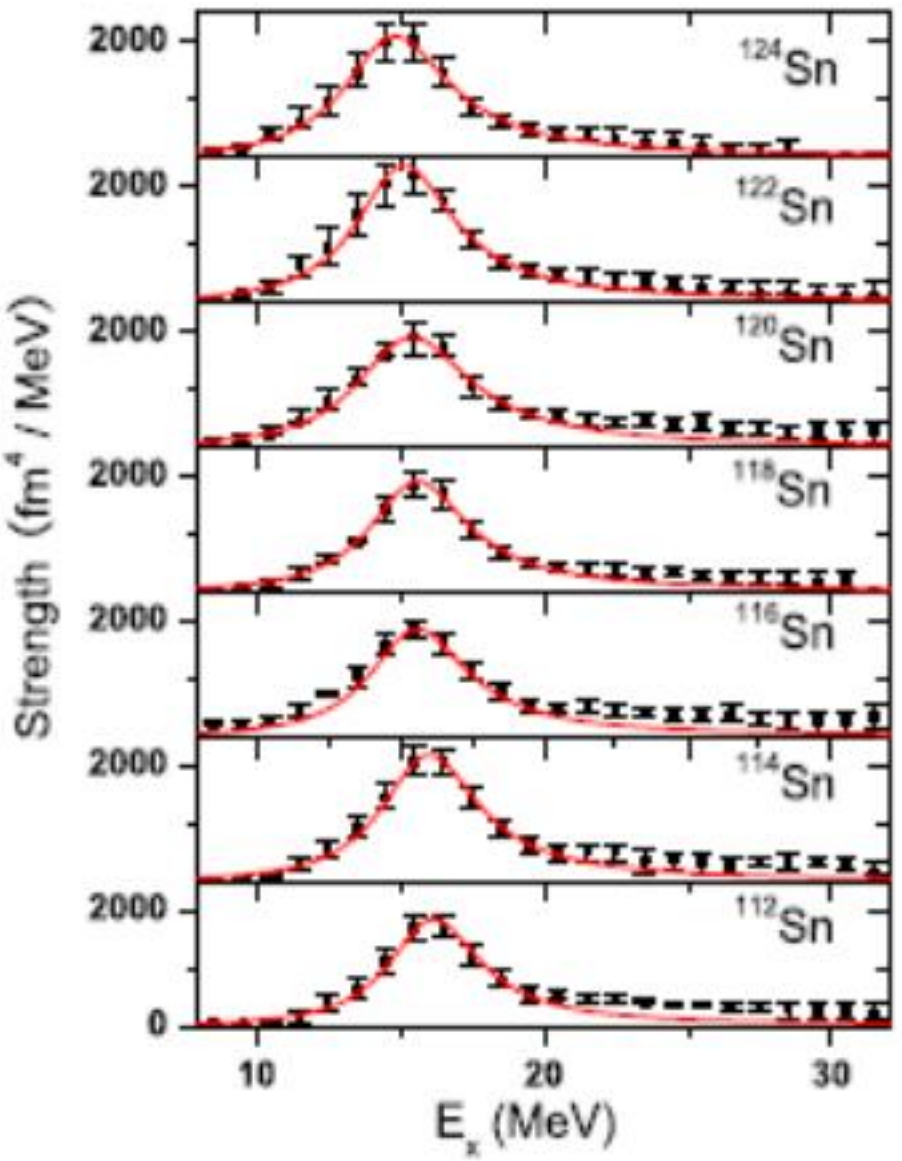

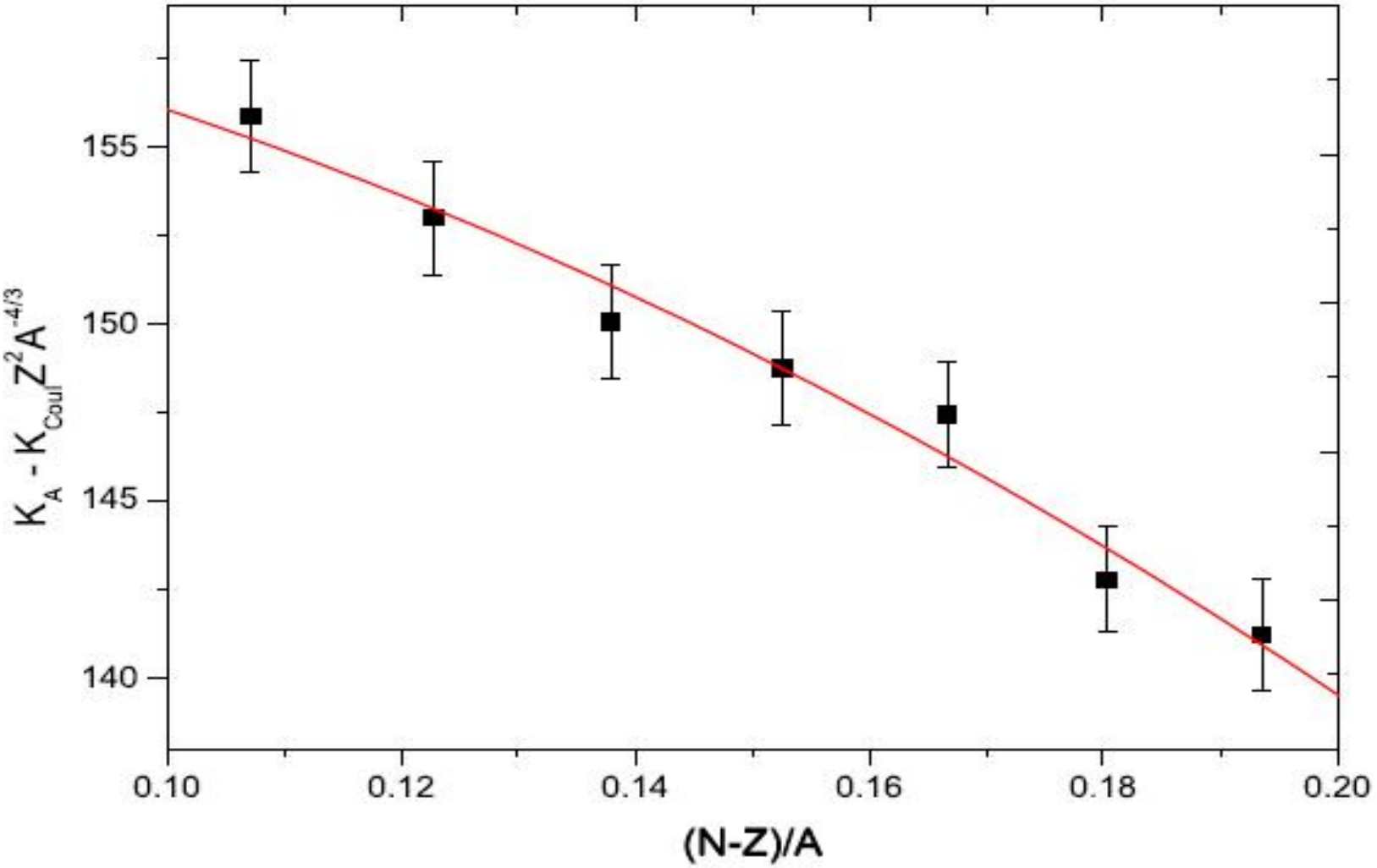

Sn isotopes $\Rightarrow$ $K_\tau = -550 \pm 100$ MeV

Outlook

Radioactive ion beams will be available at energies where it will be possible to study excitation of ISGMR and ISGDR

RIBF/RIKEN, GSI/FAIR, GANIL/SPIRAL2, FRIB/NSCL

E.g., Determine ISGMR and ISGDR in unstable Sn nuclei.

A = 106 to 134 possible

$\Rightarrow$ A more precise determination of K_τ

Nuclear structure studies with reactions in inverse kinematics

Possible at GSI/FAIR, RIKEN/RIBF, GANIL and NSCL/FRIB

(beam energies of 50-100 MeV/u are needed!)

Approach
measure the recoiling alphas

(α,α')

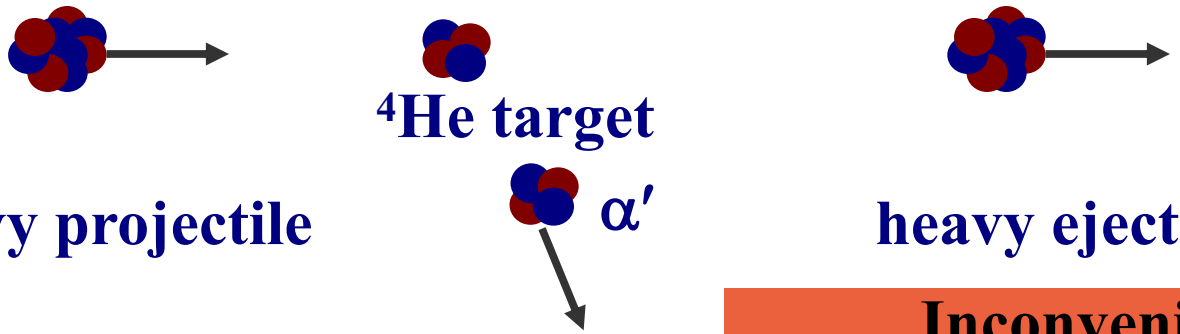

Inconvenience:
difficulty to detect the low-energy alphas

Nuclear structure studies with reactions in inverse kinematics
Challenges with exotic beams

- **Inverse kinematics**

^{56}Ni(α,α′)^{56}Ni*
α = Target
^{56}Ni = Projectile

Secondary Beam
^{56}Ni at 50 MeV/u

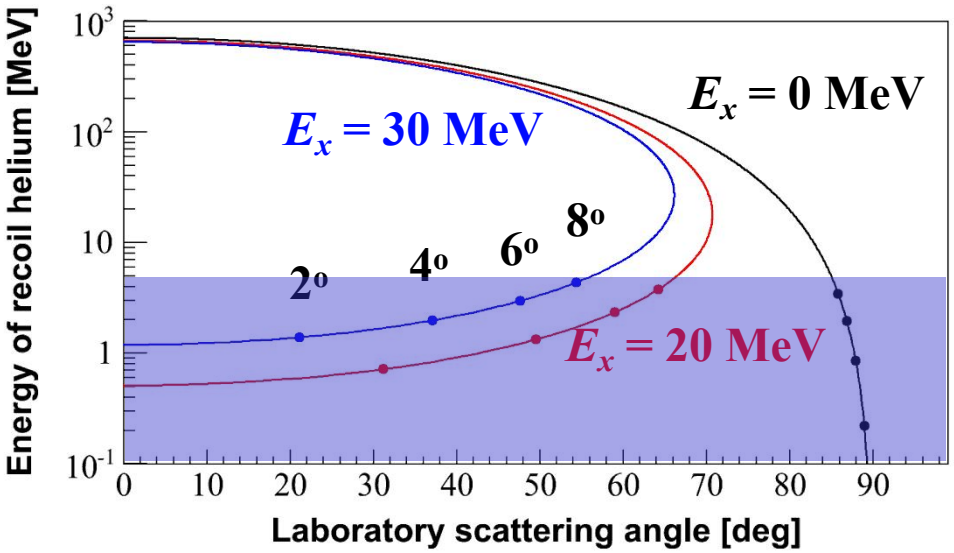

- **Intensity of exotic beams is very low (~10^4 – 10^5 pps)**
- **To get reasonable yields thick target is needed**
- **Very low energy (~ sub MeV) recoil particle will not come out of the thick target**

Active target

A gas detector where the target gas also acts as a detector

Advantages

- **Good angular coverage**
- **Effective target thickness can be increased without much loss of resolution**
- **Detection of very low-energy recoil particle is possible**

Disadvantages

- **Low beam intensities (~10^4 – 10^5 pps)**
- **Very small recoil energies for low q**

MAYA active-target detector at GANIL

Primary Beam
^{58}Ni at 75 MeV/u

Primary Target: ^{9}Be
(thickness 525.6 µm)

Secondary Beam
^{56}Ni at 50 MeV/u

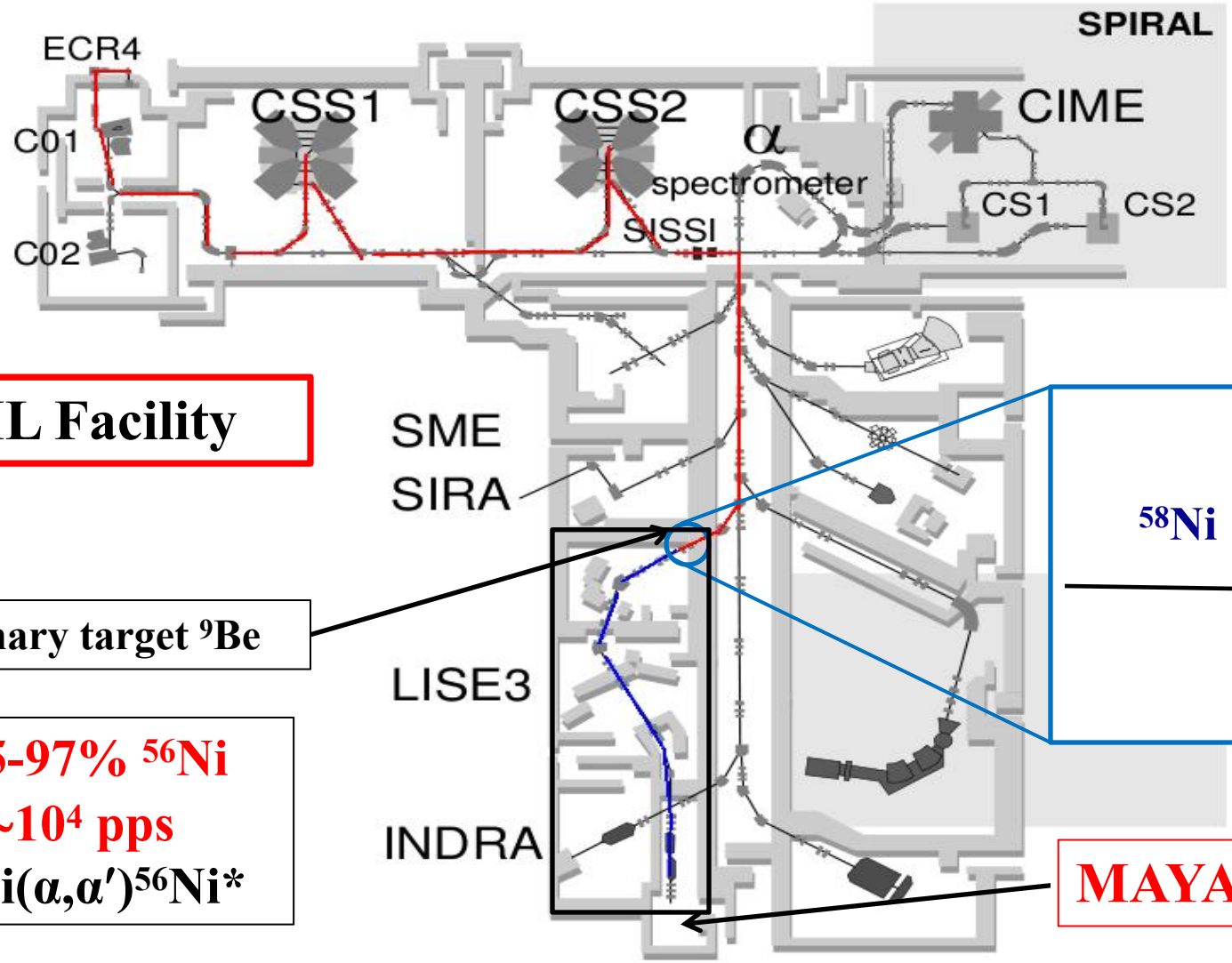

GANIL Facility

Primary target ^{9}Be

95-97% ^{56}Ni
~10^4 pps
^{56}Ni(α,α′)^{56}Ni*

MAYA setup

MAYA setup (I)

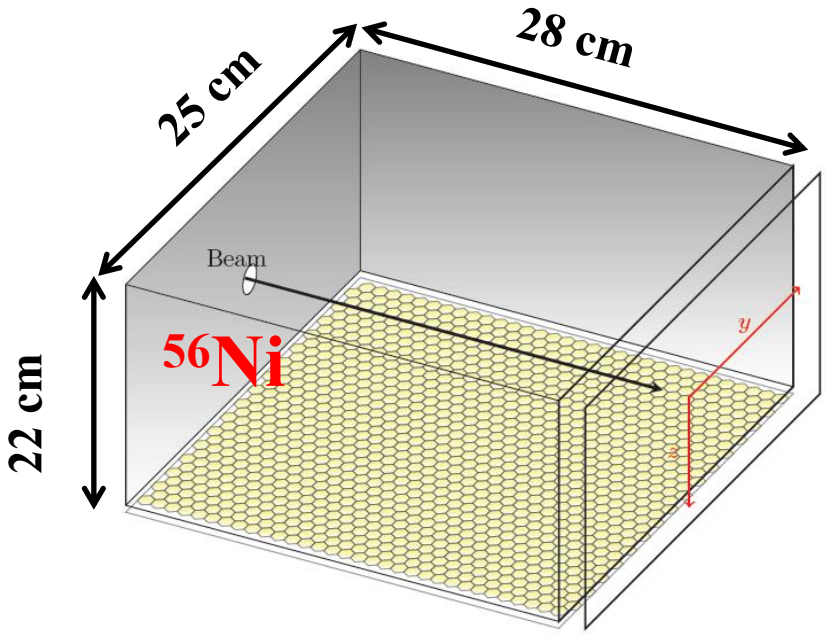

500 mbar
95% He and 5% CF_4

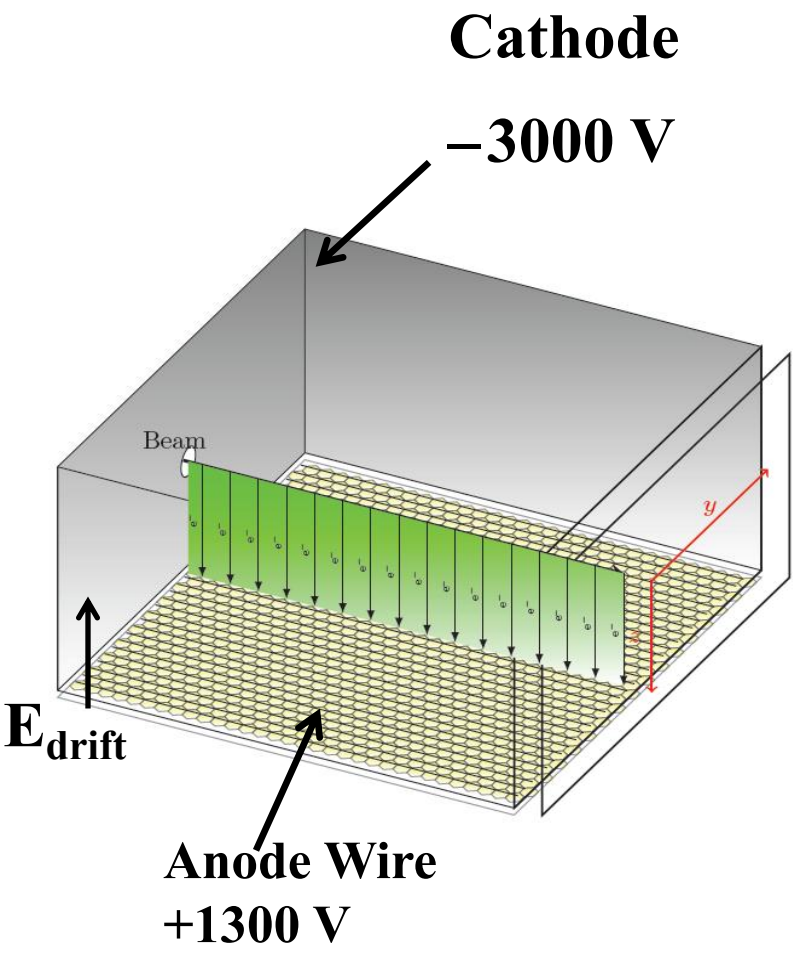

MAYA setup (II): Electrostatic mask

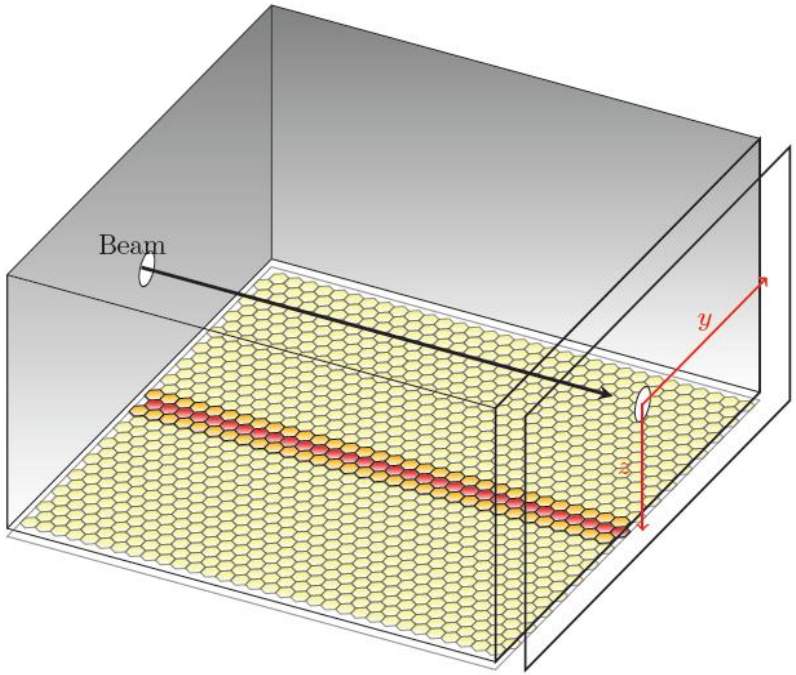

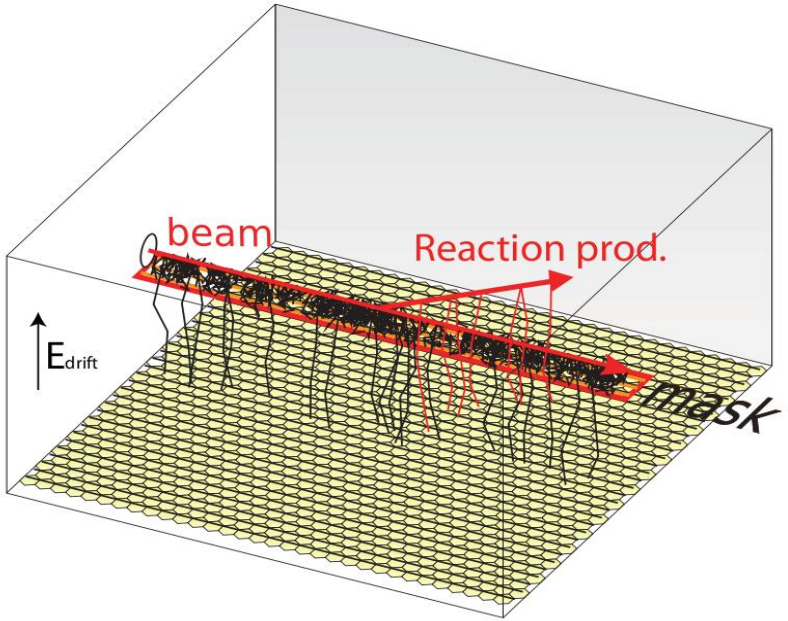

MAYA setup (III): Si/CsI telescope

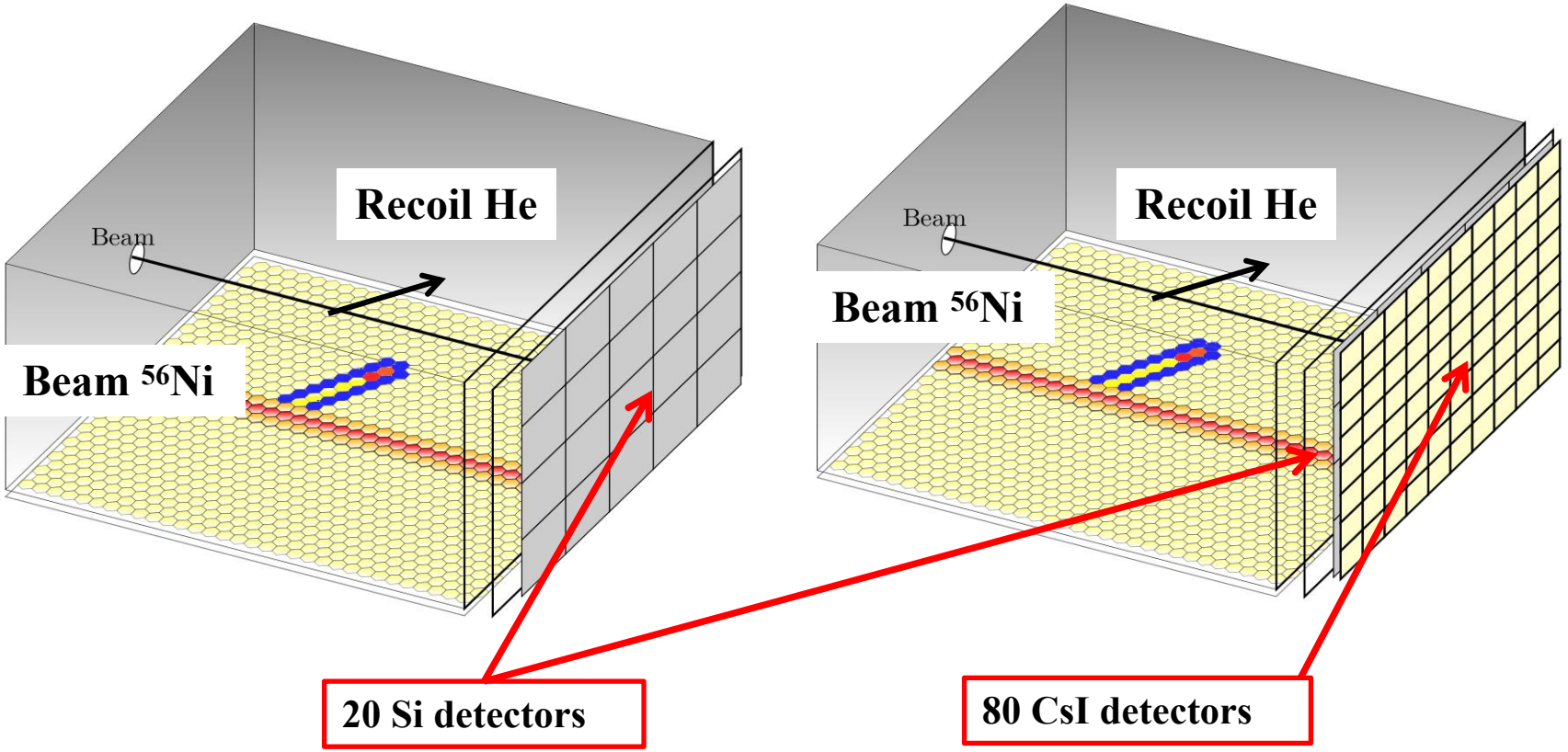

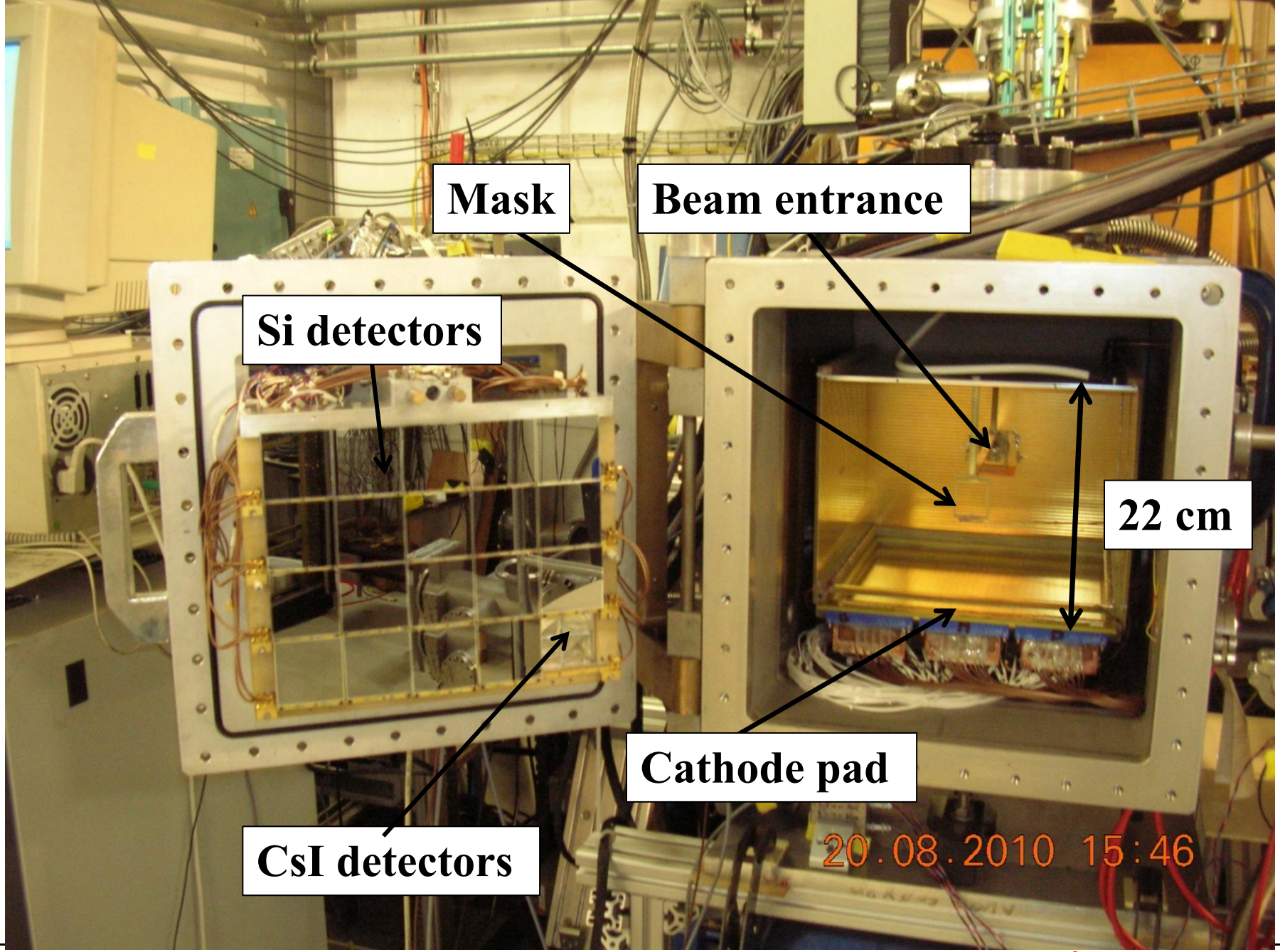
Mask
Beam entrance
Si detectors
22 cm
Cathode pad
CsI detectors
20.08.2010 15:46

Cathode pad in MAYA

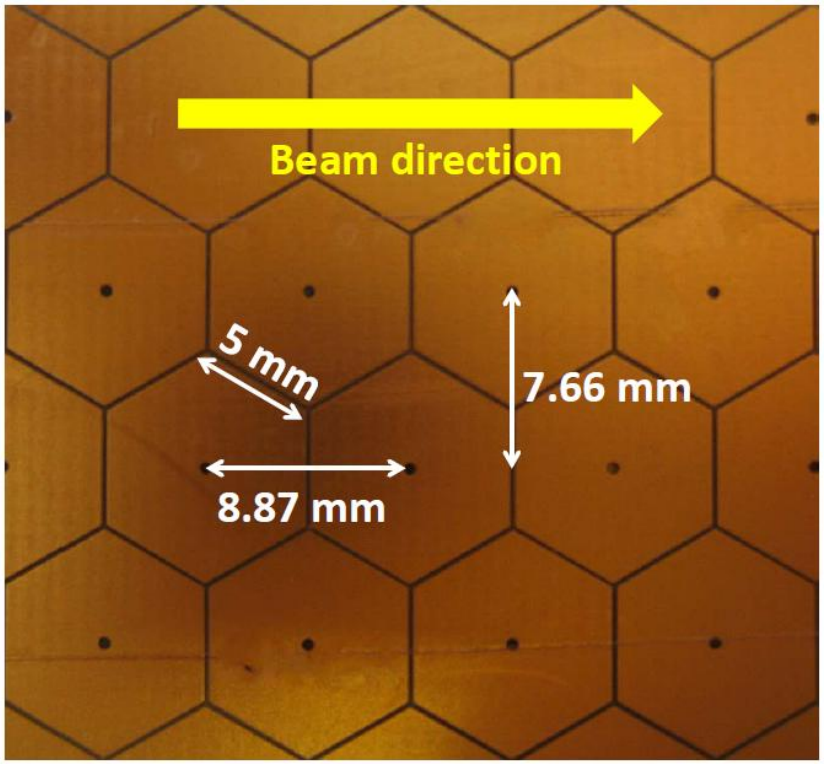

MAYA

Basics of kinematics reconstruction inside MAYA

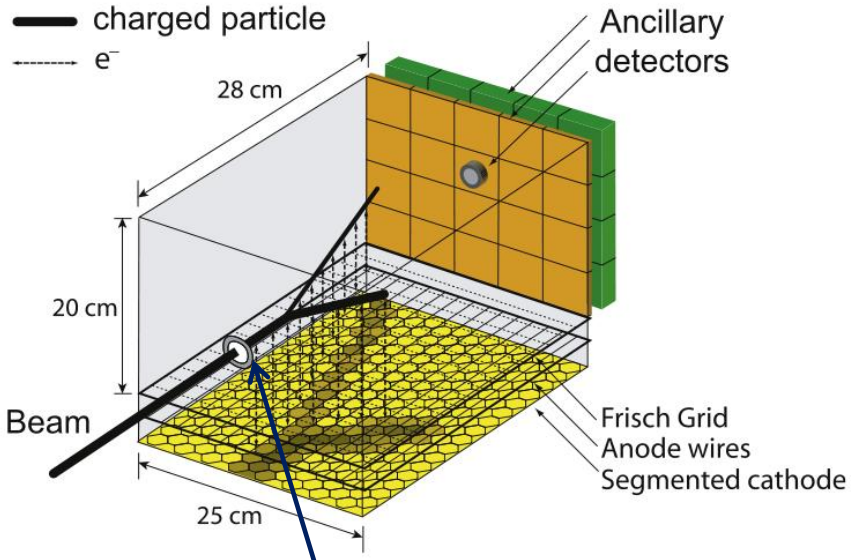

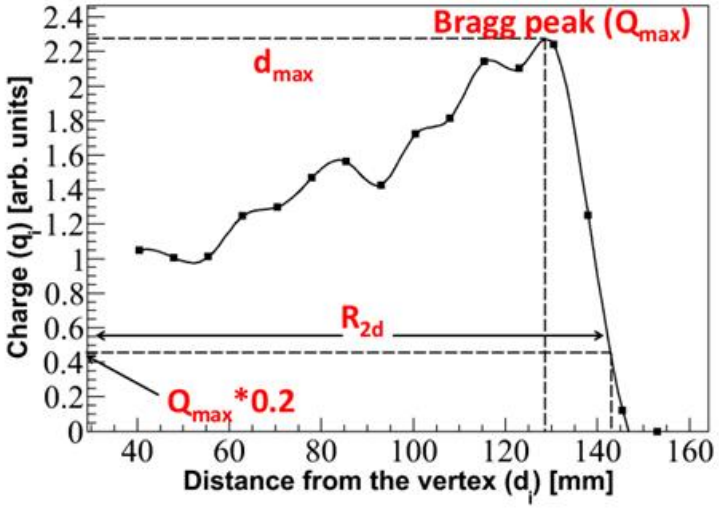

Timing information from Amplification wires

$$R_{2d} \rightarrow R_{3d}\,,\ \theta_{2d} \rightarrow \theta_{3d}$$

Range ⟶ Energy (SRIM)

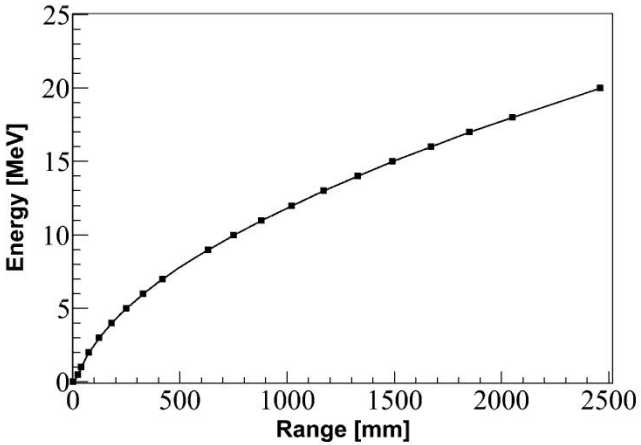

Track reconstruction: Different regions on the cathode pad

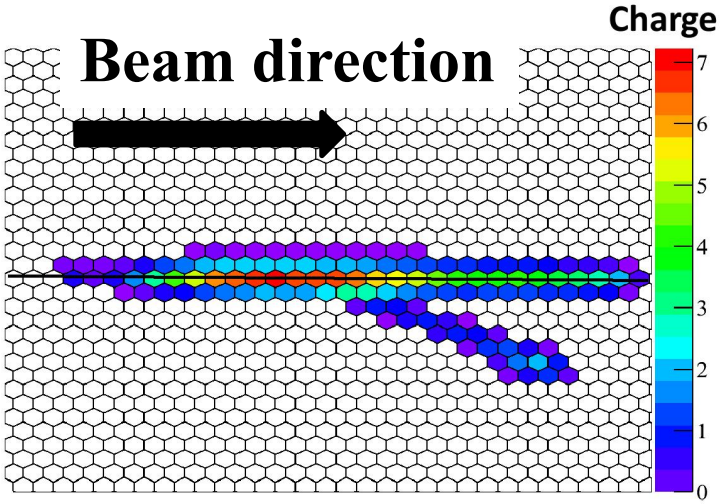

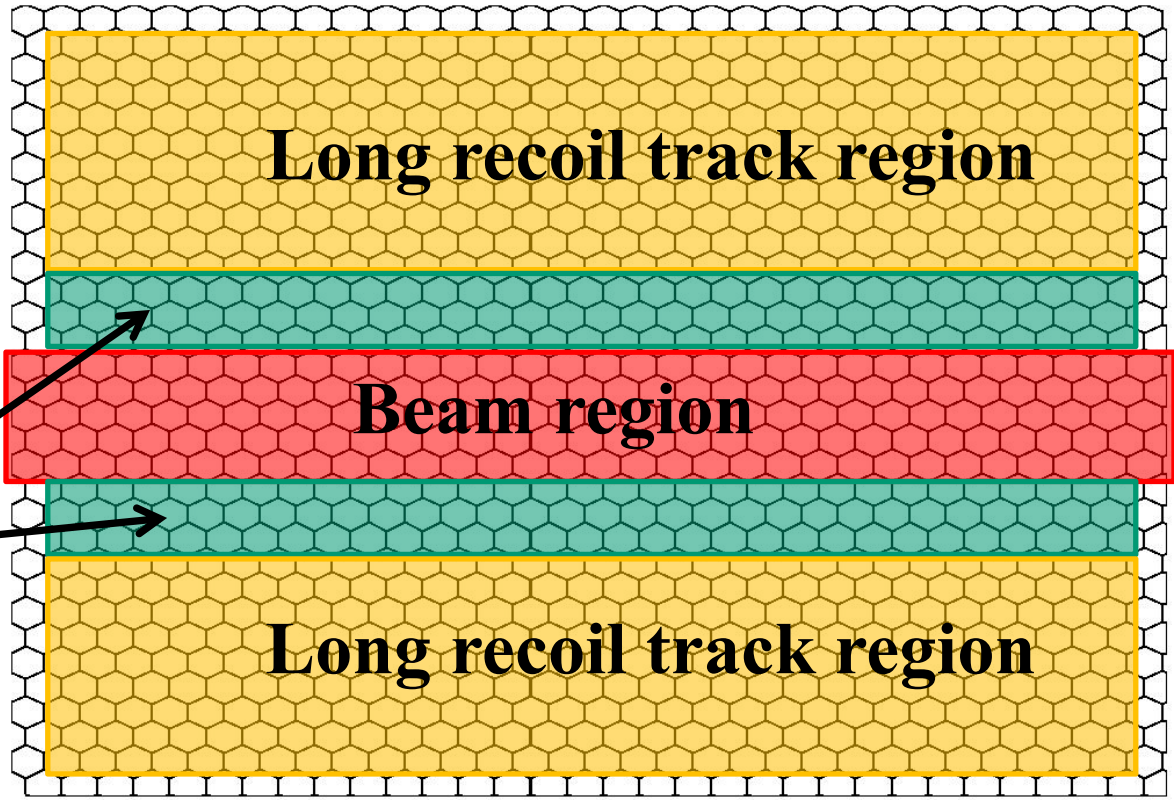

Short recoil track region

Charge projection along the symmetry axis of a hexagon

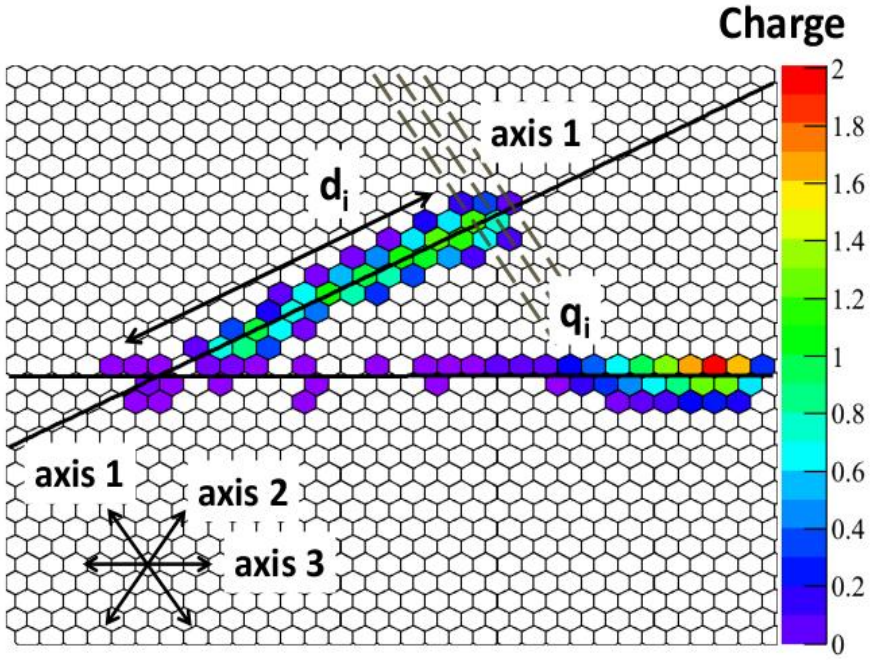

Beam direction

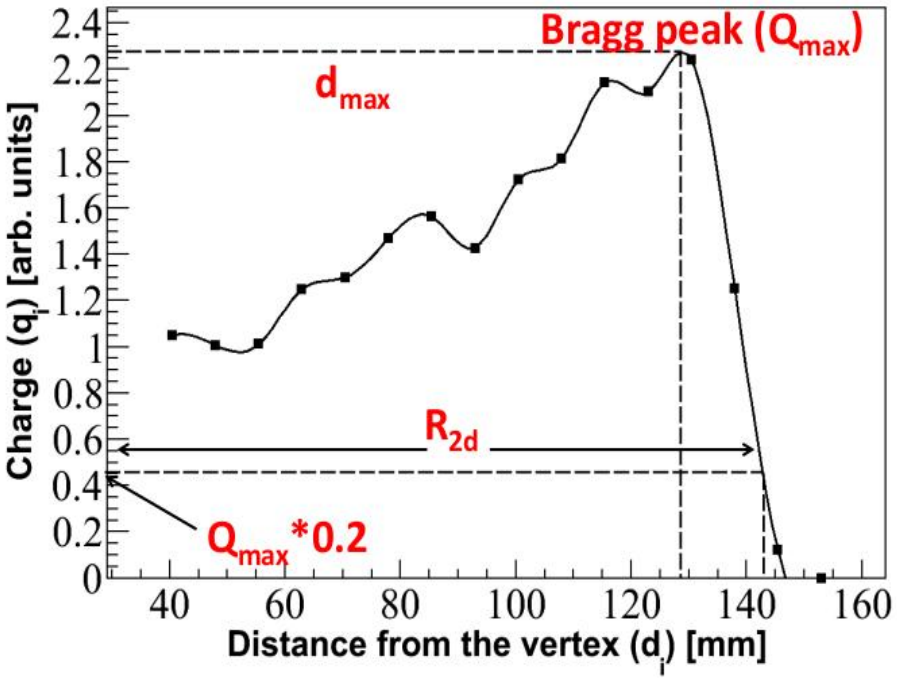

3rd dimension from timing information of the anode wires

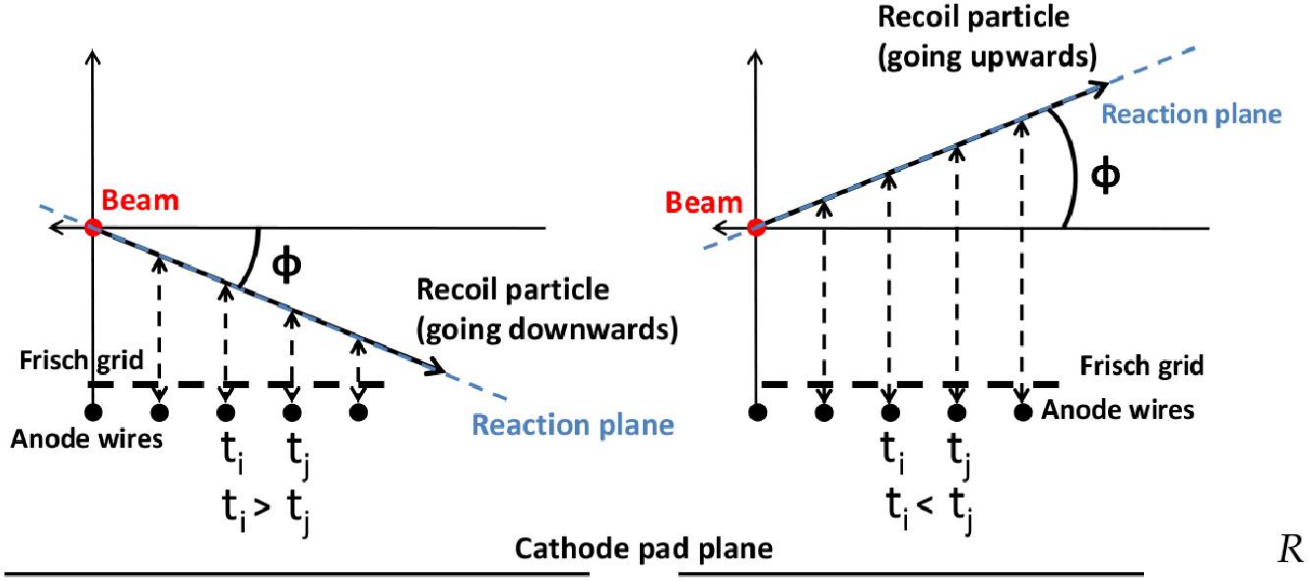

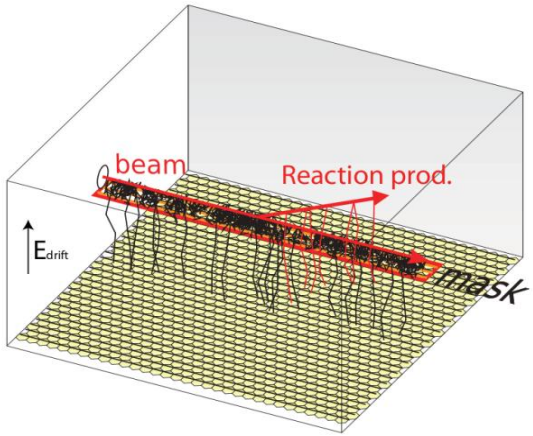

$$R = R_{2d}\sqrt{1 + \sin^2\theta_{2d}\tan^2\phi}$$

Range → Energy

$$\cos\theta = \frac{\cos\theta_{2d}}{\sqrt{1 + \sin^2\theta_{2d}\tan^2\phi}}$$

Kinematics plot

Data

$^{56}Ni(\alpha,\alpha')^{56}Ni^*$

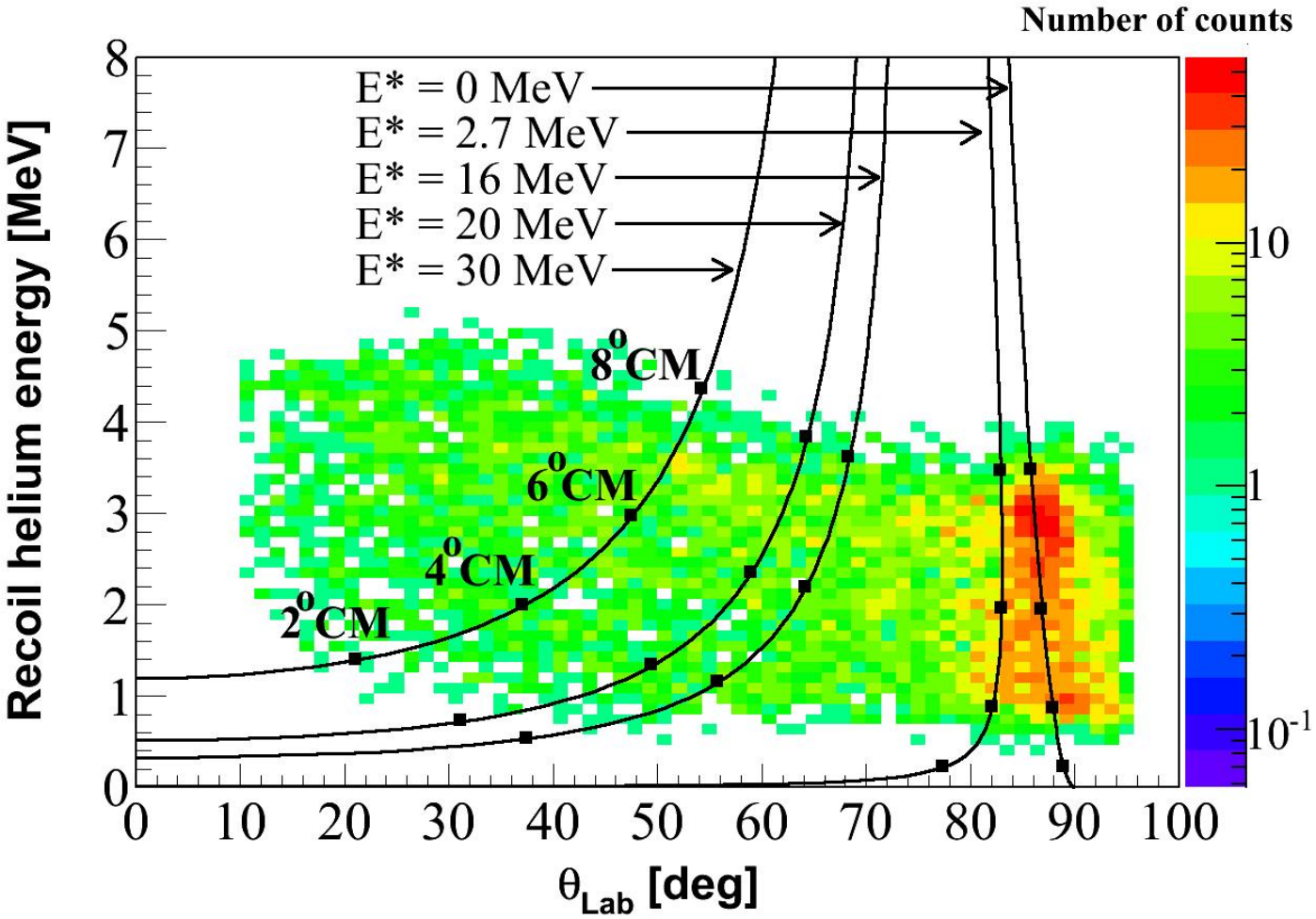

Efficiency (reconstruction and geometric) plot from simulation

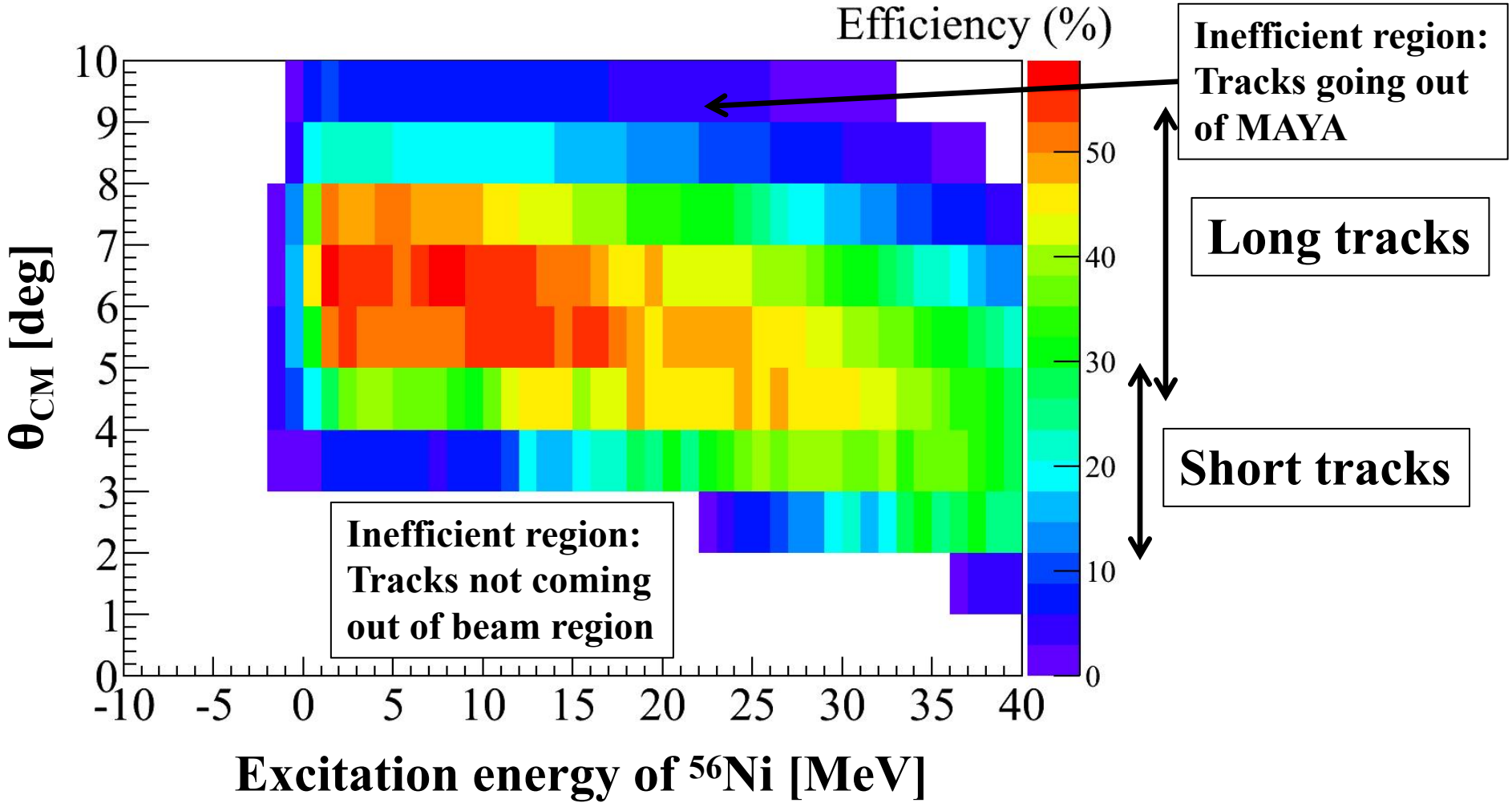

Efficiency correction

Data (Not efficiency corrected)

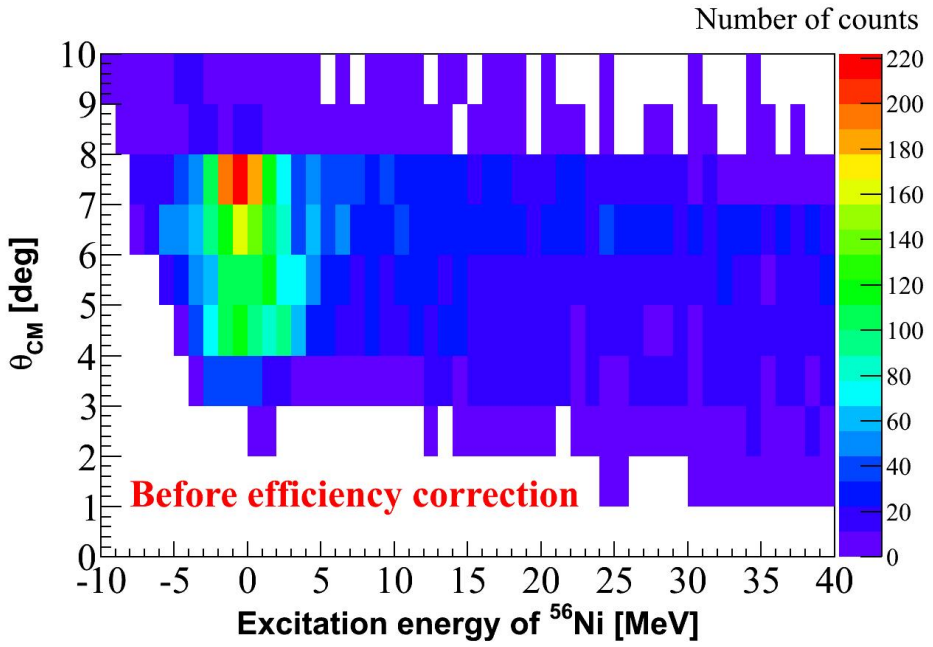

Data (Efficiency corrected)

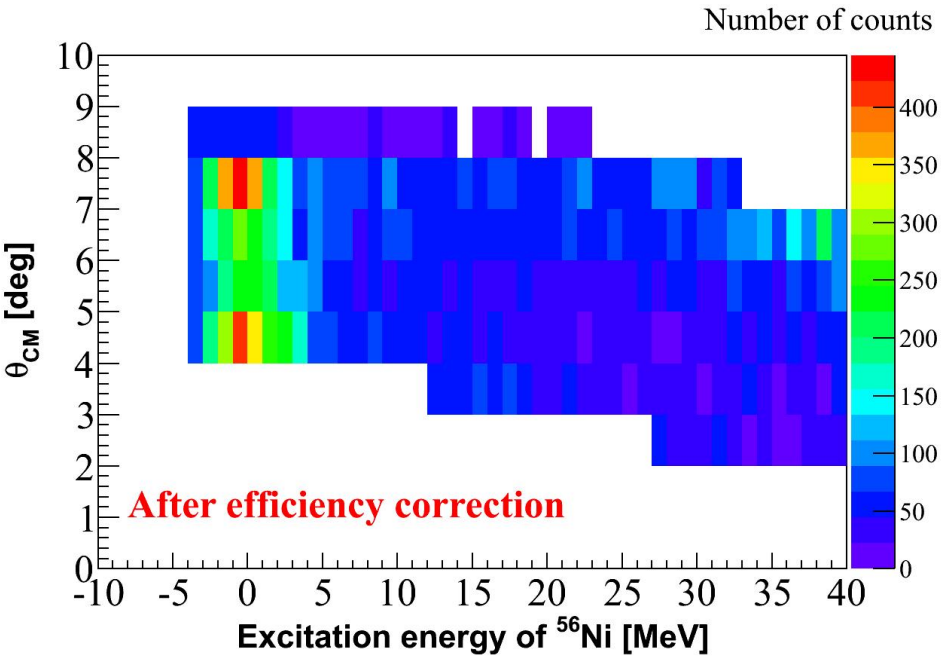

Data (Efficiency corrected)

Peak fitting method

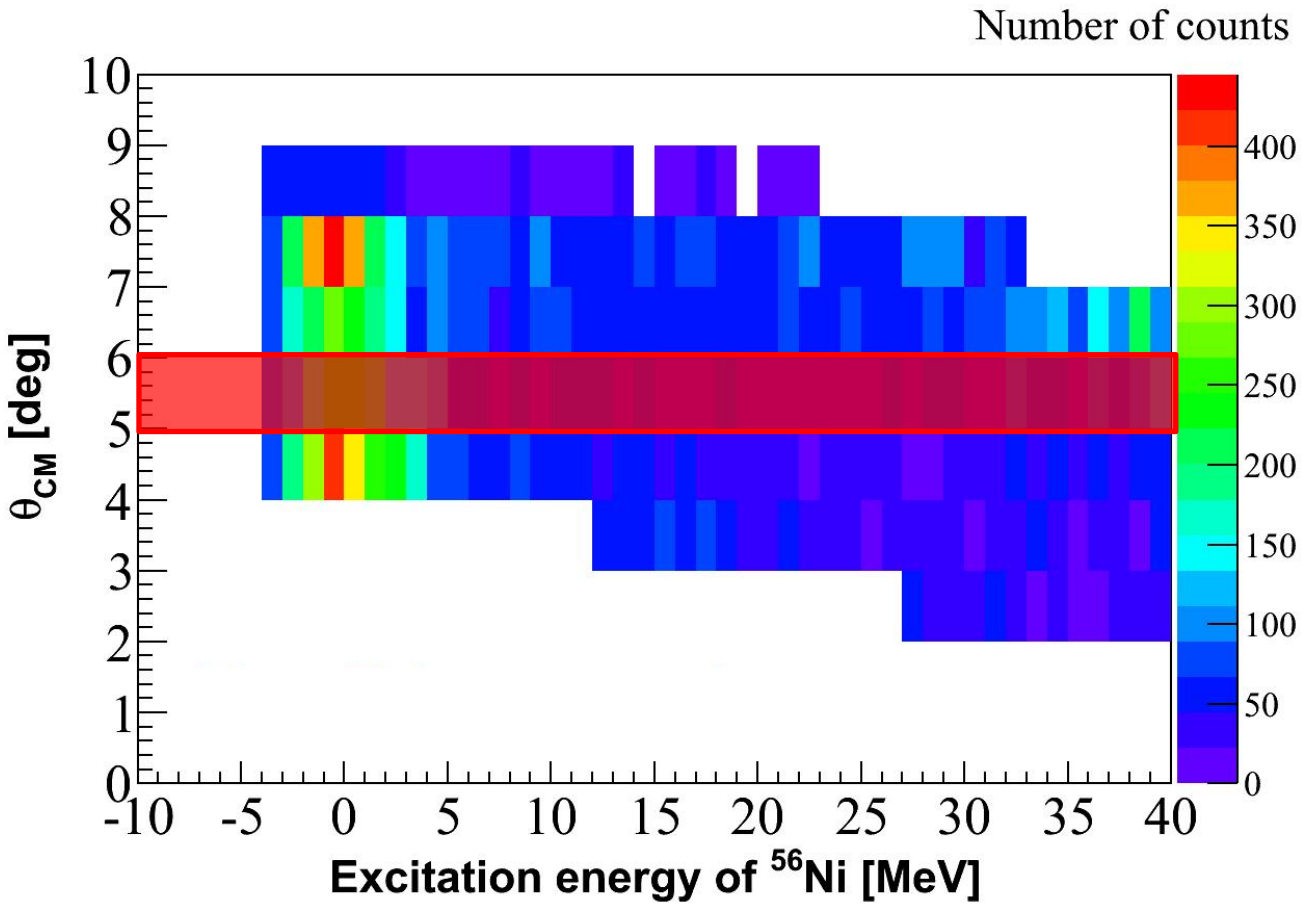

Peak fitting method

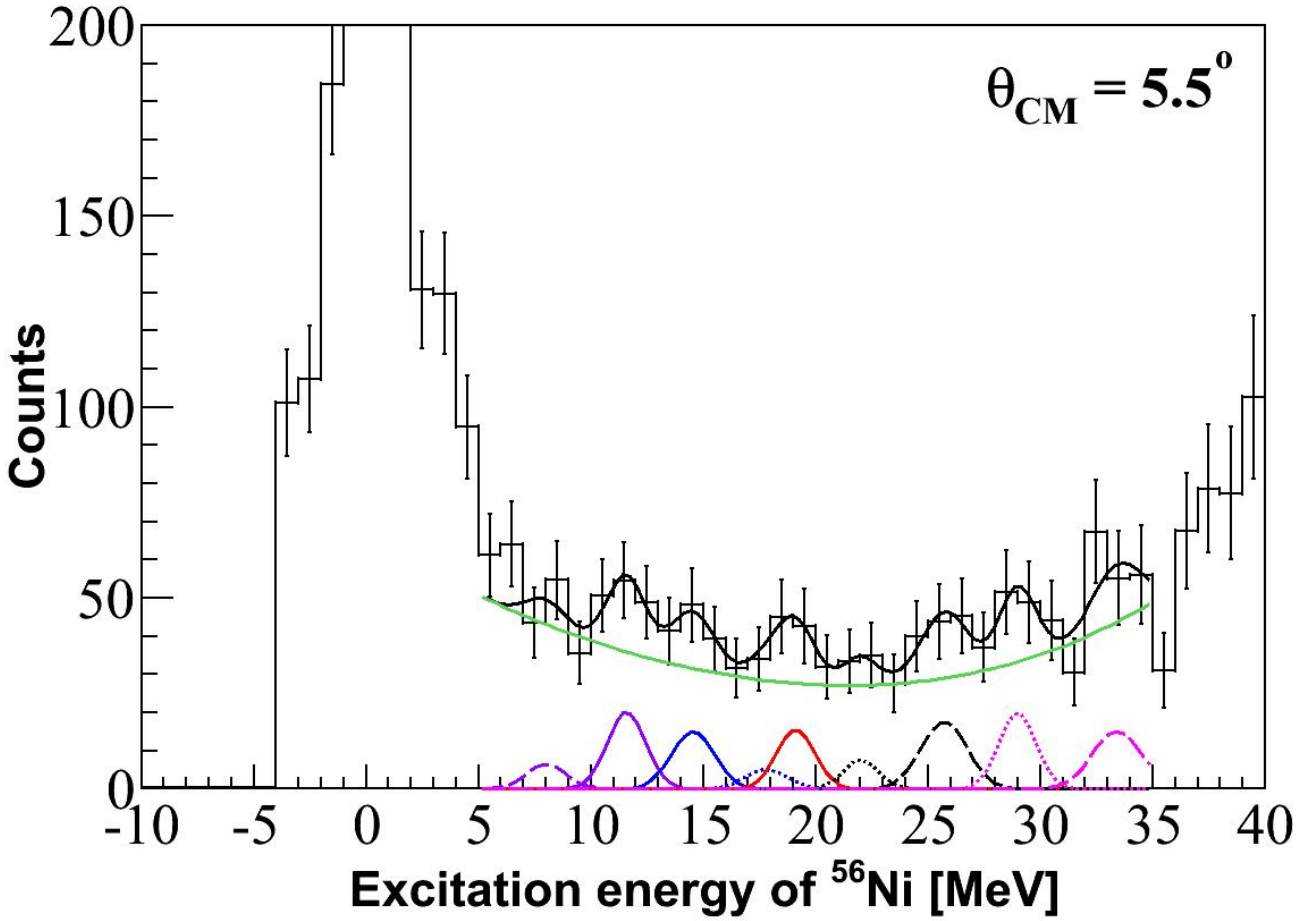

Angular distribution of the Gaussian peaks

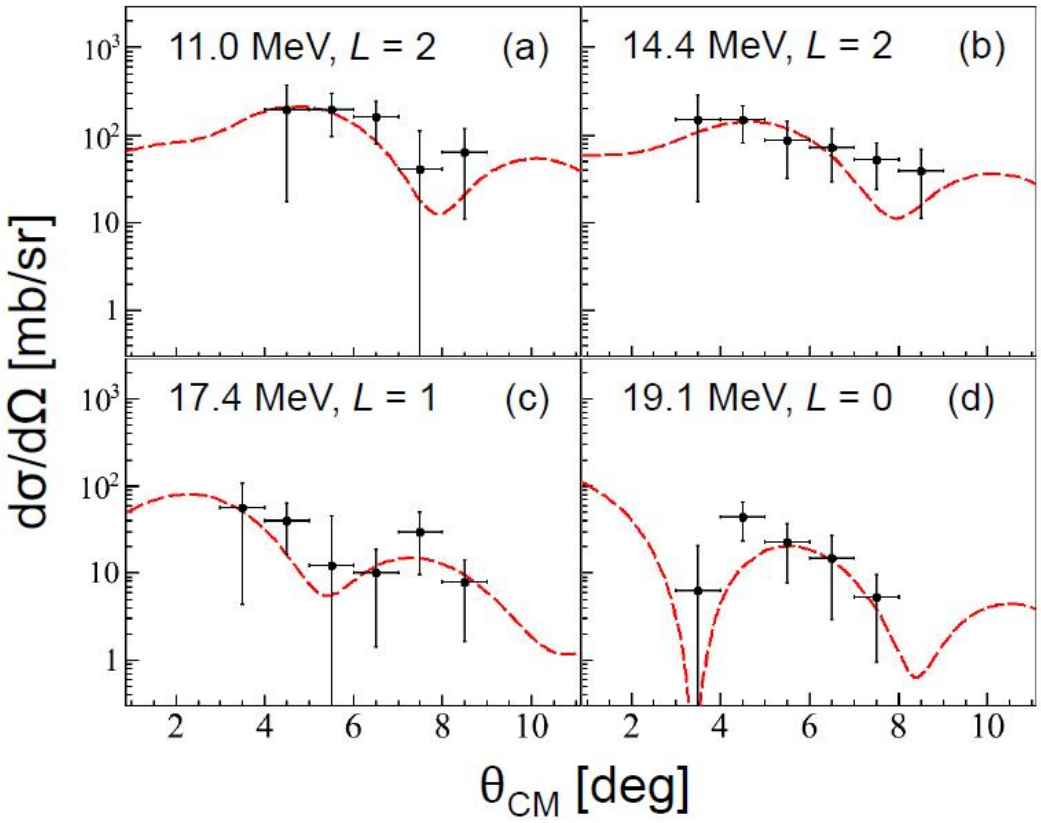

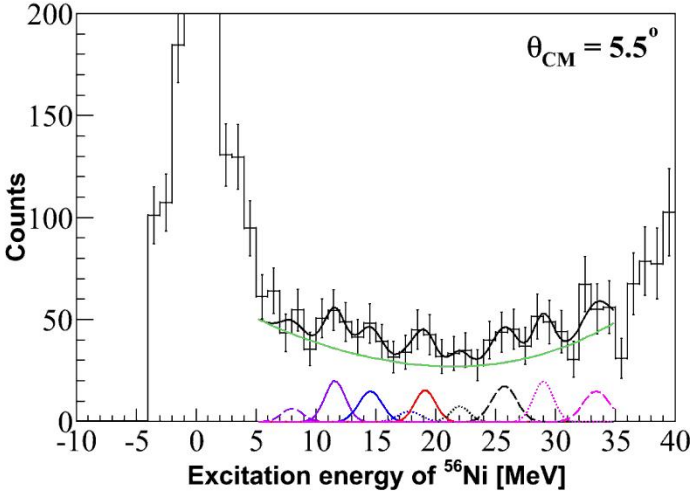

Multipole Decomposition Analysis (MDA)

Data (Efficiency corrected)

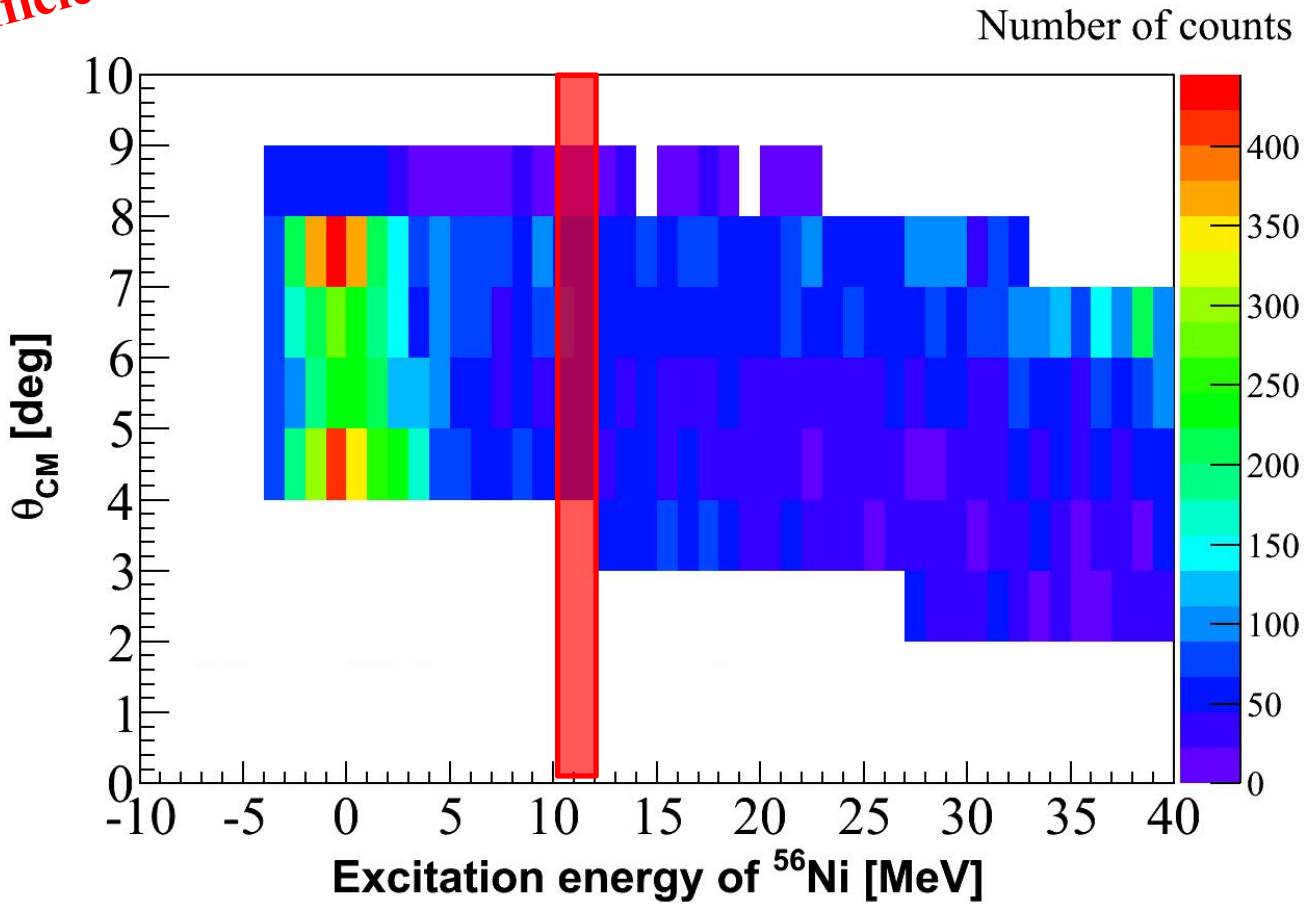

$$\left.\frac{d^2\sigma}{d\Omega\, dE}(\theta_{CM}, E^*)\right|_{exp} = \sum_{L=0}^{L=3} a_L(E^*) \left.\frac{d^2\sigma_L}{d\Omega\, dE}(\theta_{CM}, E^*)\right|_{theory}$$

Coefficient represents the sum-rule strength for *L* and *E**

Experimental angular distribution for a given energy interval

Angular distribution obtained from DWBA calculations for a given energy interval and multipolarity

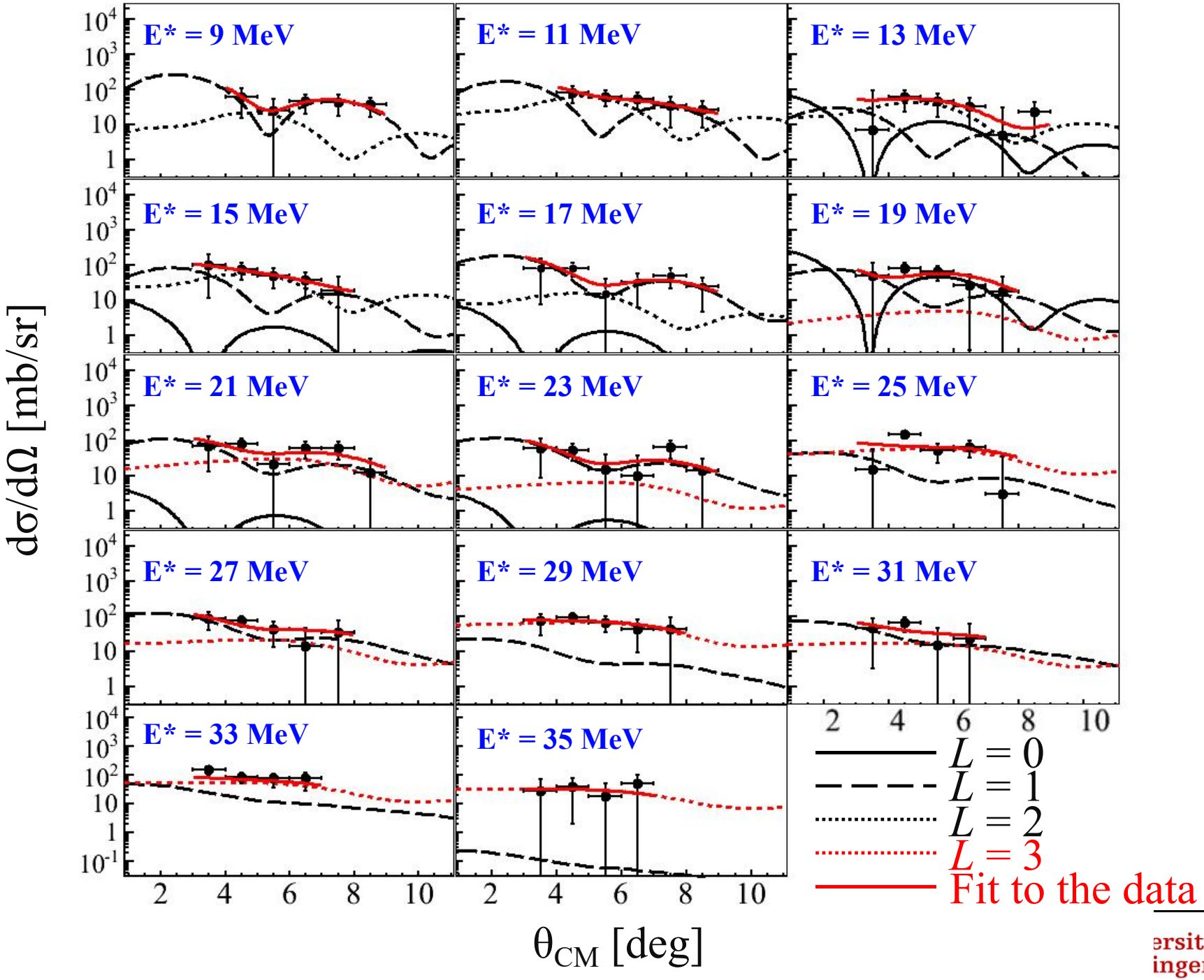
E* = 9 MeV
E* = 11 MeV
E* = 13 MeV
E* = 15 MeV
E* = 17 MeV
E* = 19 MeV
E* = 21 MeV
E* = 23 MeV
E* = 25 MeV
E* = 27 MeV
E* = 29 MeV
E* = 31 MeV
E* = 33 MeV
E* = 35 MeV
dσ/dΩ [mb/sr]
θCM [deg]
L = 0
L = 1
L = 2
L = 3
Fit to the data

$L = 0,\ T = 0$ (ISGMR)

EWSR obtained from MDA analysis

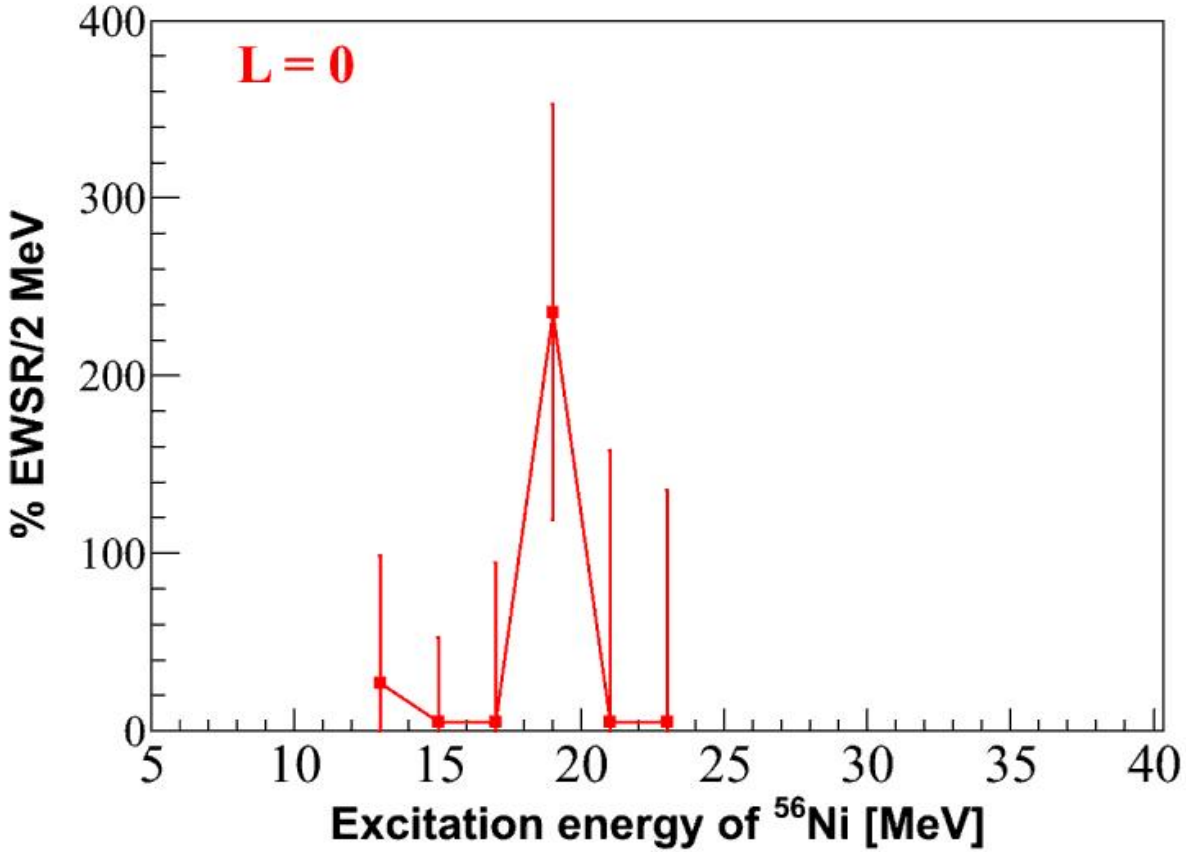

$L = 0$, $T = 0$ (ISGMR)

Reaction	Gaussian fitting		MDA	
	E* [MeV]	FWHM [MeV]	E* [MeV]	Width (rms) [MeV]
^{56}Ni(α,α')^{56}Ni* (this work)	19.1±0.5	2.0±0.3	18.4±1.8	2.0±1.2
^{56}Ni(d,d')^{56}Ni*	19.5±0.3	5.2	19.3±0.5	2.3
^{58}Ni(α,α')^{58}Ni*	18.43±0.15	7.41±0.13	$19.2^{+0.44}_{-0.19}$	$4.89^{+1.05}_{-0.31}$
^{58}Ni(α,α')^{58}Ni*	-	-	$19.9^{+0.7}_{-0.8}$	-
^{60}Ni(α,α')^{60}Ni*	17.62±0.15	7.55±0.13	$18.04^{+0.35}_{-0.23}$	$4.5^{+0.97}_{-0.22}$
^{68}Ni(α,α')^{68}Ni*	21.1±1.9	1.3±1.0	23.4	6.5

S. Bagchi *et al.*, Phys. Lett. B751 (2015) 371; C. Monrozeau *et al.*, Phys. Rev. Lett. 100 (2008) 042501; M. Vandebrouck *et al.*, Phys. Rev. Lett. 113 (2014) 032504; Y.-W. Lui *et al.*, Phys. Rev. C 73 (2006) 014314.

Summary & conclusion:

- **Inelastic α-particle scattering is suitable for isoscalar excitations.**
- **First measurement of the isoscalar responses of ^{56}Ni via inelastic α-particle scattering.**
- **Active target techniques can be used to study the properties of unstable nuclei.**
- ***L* = 0 mode:**

  Centroid: 19.1 ± 0.5 MeV (Peak-fitting method)

  18.4 ± 1.8 MeV (MDA)
- **Low-lying component of the ISGDR.**

GSI Storage Ring

Experimental Storage Ring

Luminosity:
$10^{26} – 10^{27}$ $cm^{-2}s^{-1}$

EPJ Web Conf. 66 (2014) 03093

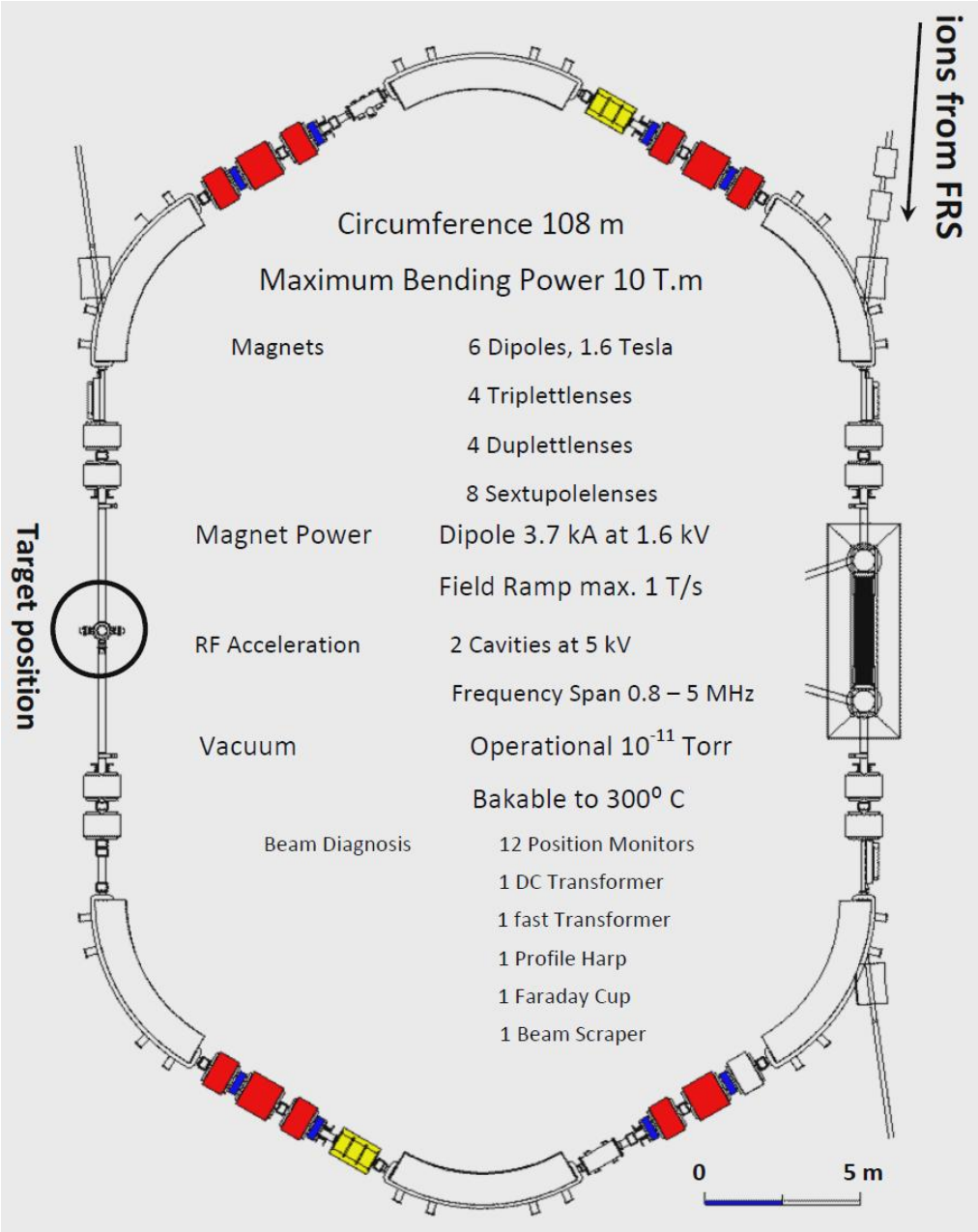

Advantages and disadvantages of storage-ring experiments

Advantages:
Large intensities in the ring
Little energy loss in the target
No target window (no background)
High resolution of the beam (electron cooling)
Forward focusing for high-energy particles
Low-energy threshold

Disadvantages:
Ultra high vacuum
Very small recoil energies for low q
Thin targets

Prototype of EXL (EXotic nuclei studied in Light-ion induced reactions at the (N)ESR storage ring) detector at ESR

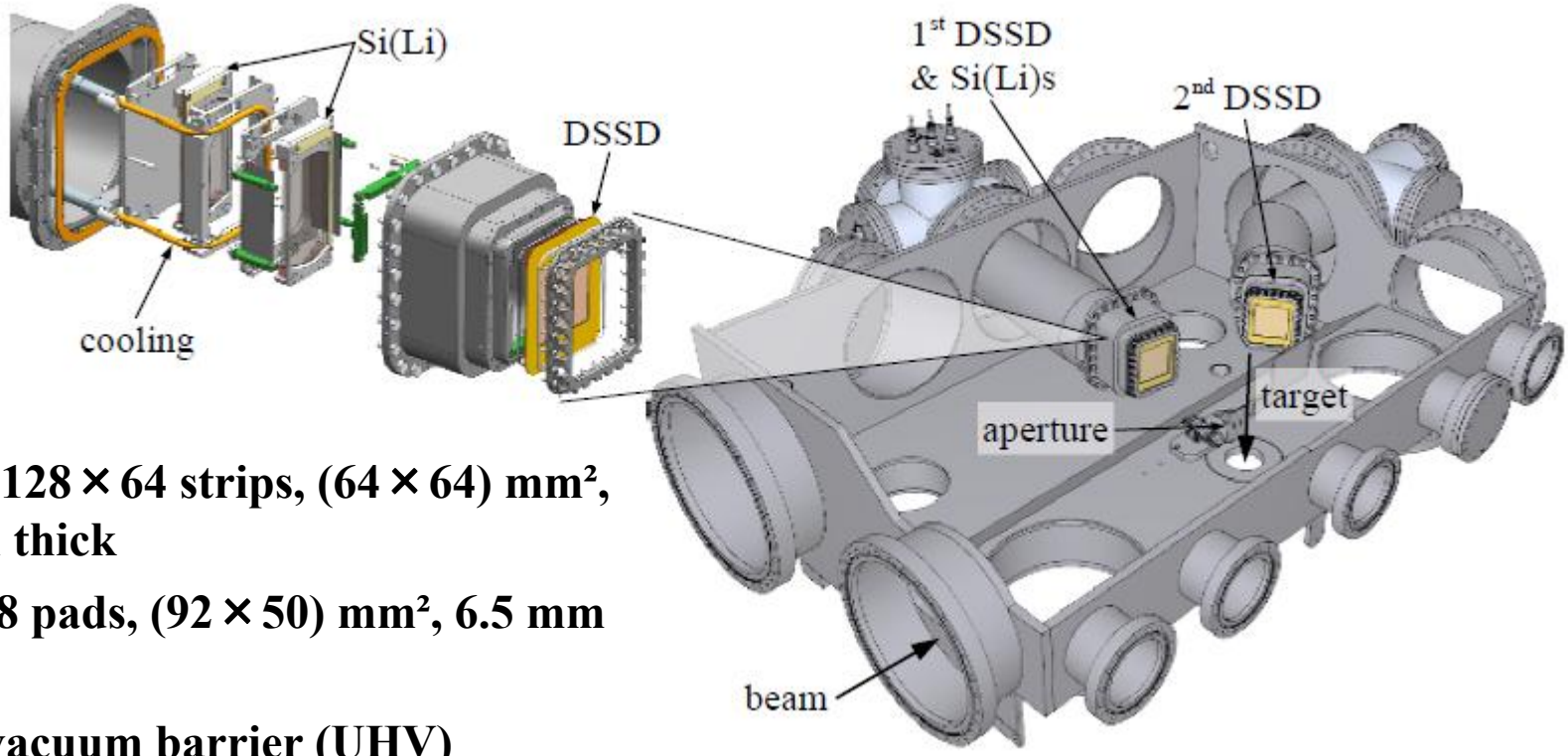

- **DSSD: 128 × 64 strips, (64 × 64) mm², 285 µm thick**
- **Si(Li): 8 pads, (92 × 50) mm², 6.5 mm thick**
- **active vacuum barrier (UHV)**
- **moveable aperture to improve angular resolution**

$73° < \theta_{lab} < 88°$ for DSSD1, and
$27° < \theta_{lab} < 38°$ for DSSD2

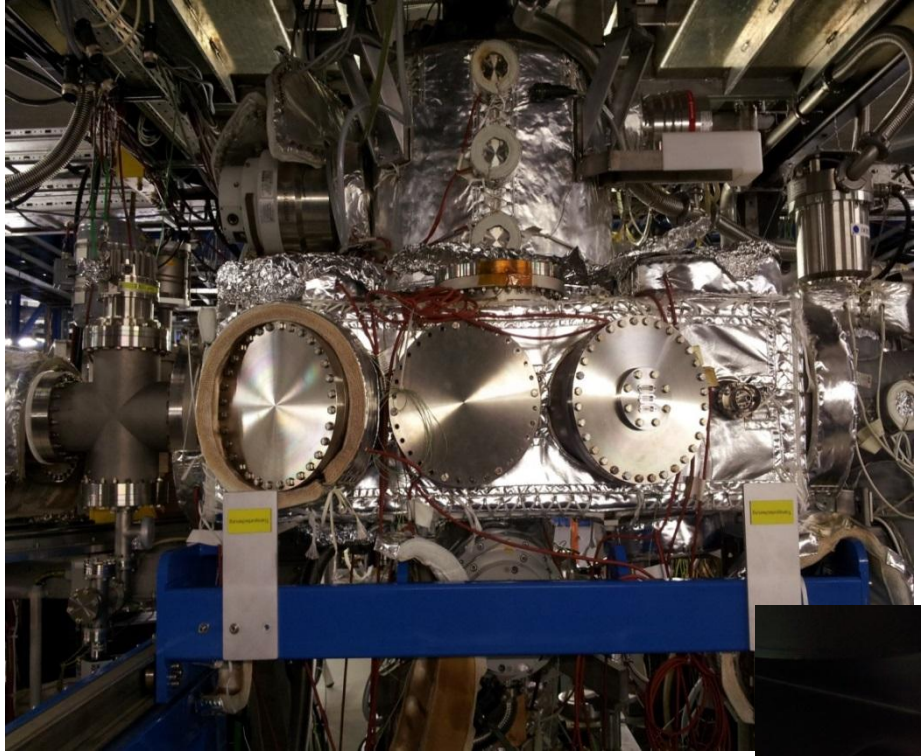

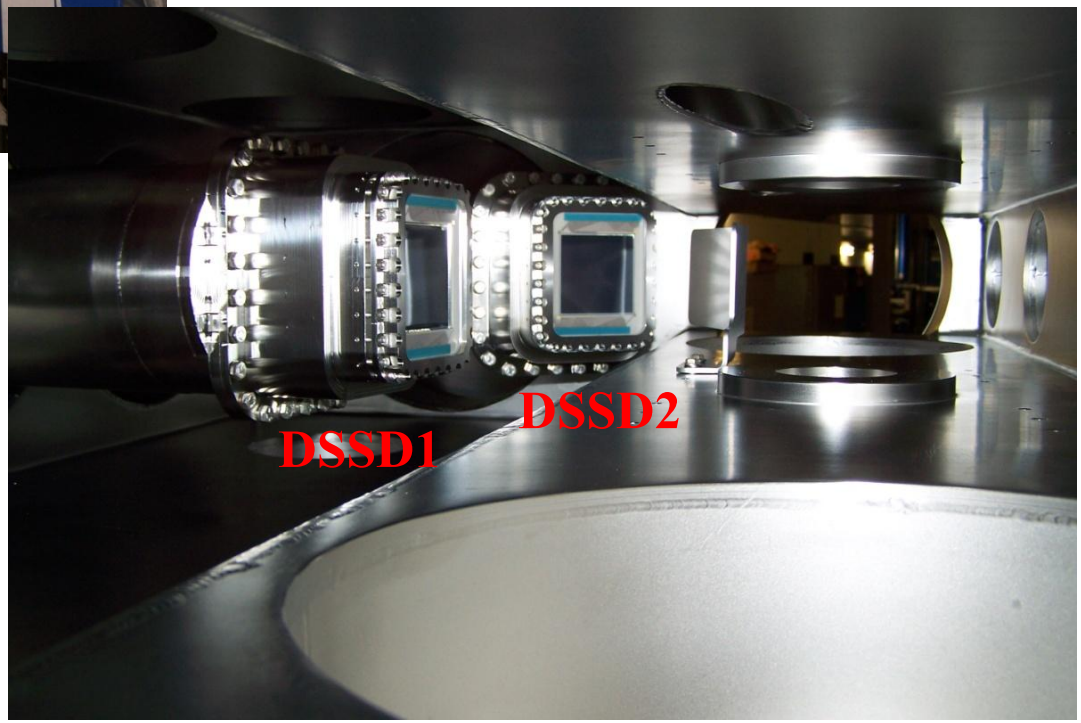
DSSD1
DSSD2

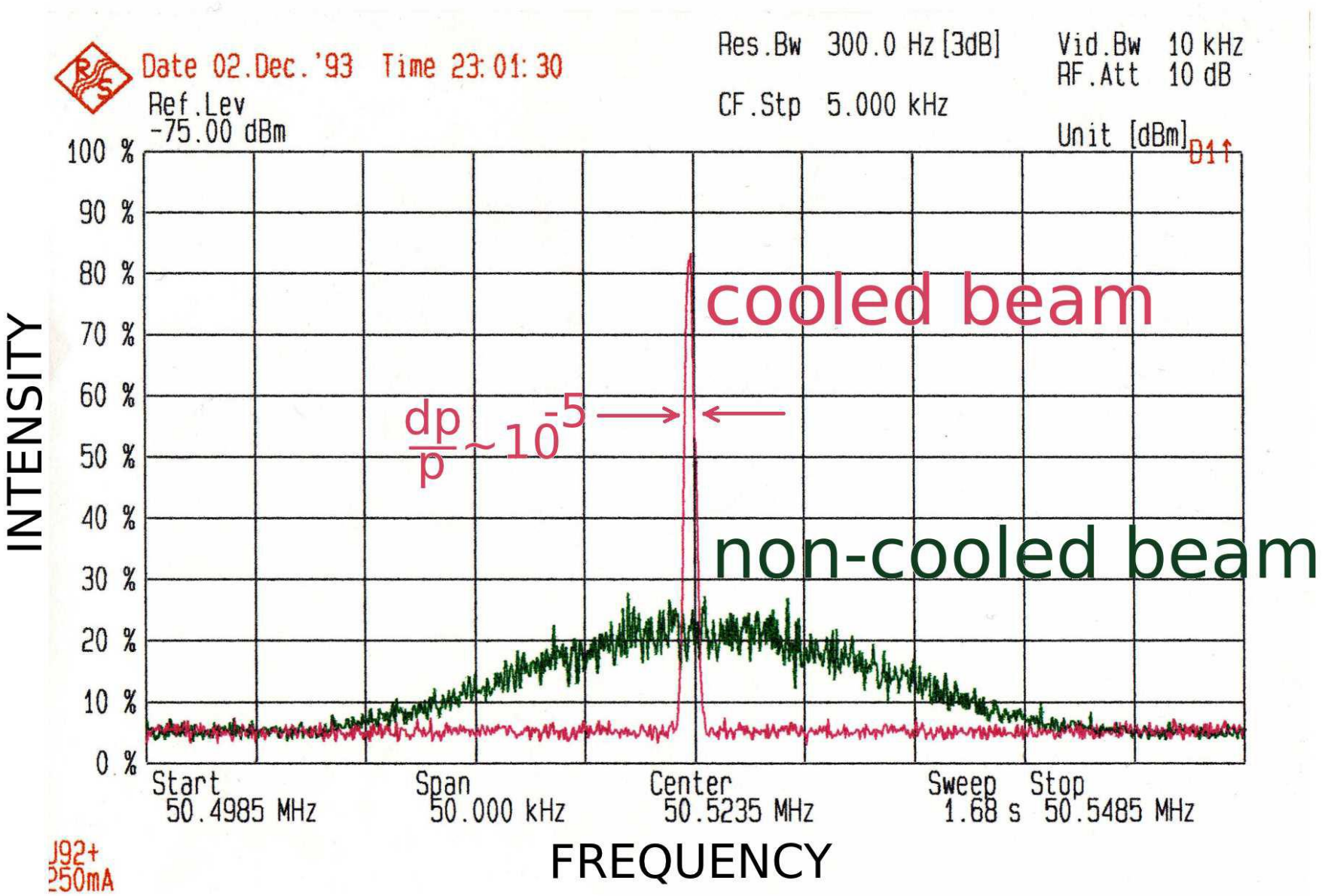
Date 02.Dec.'93 Time 23:01:30
Res.Bw 300.0 Hz [3dB]
Vid.Bw 10 kHz
RF.Att 10 dB
CF.Stp 5.000 kHz
Ref.Lev
-75.00 dBm
Unit [dBm]
D1↑
100 %
90 %
80 %
70 %
60 %
50 %
40 %
30 %
20 %
10 %
0 %
cooled beam
dp/p ~ 10^-5
non-cooled beam
INTENSITY
Start
50.4985 MHz
Span
50.000 kHz
Center
50.5235 MHz
Sweep
1.68 s
Stop
50.5485 MHz
FREQUENCY
J92+
250mA

Elastic alpha scattering at 100 MeV/nucleon
Ph.D. work of J.C. Zamora

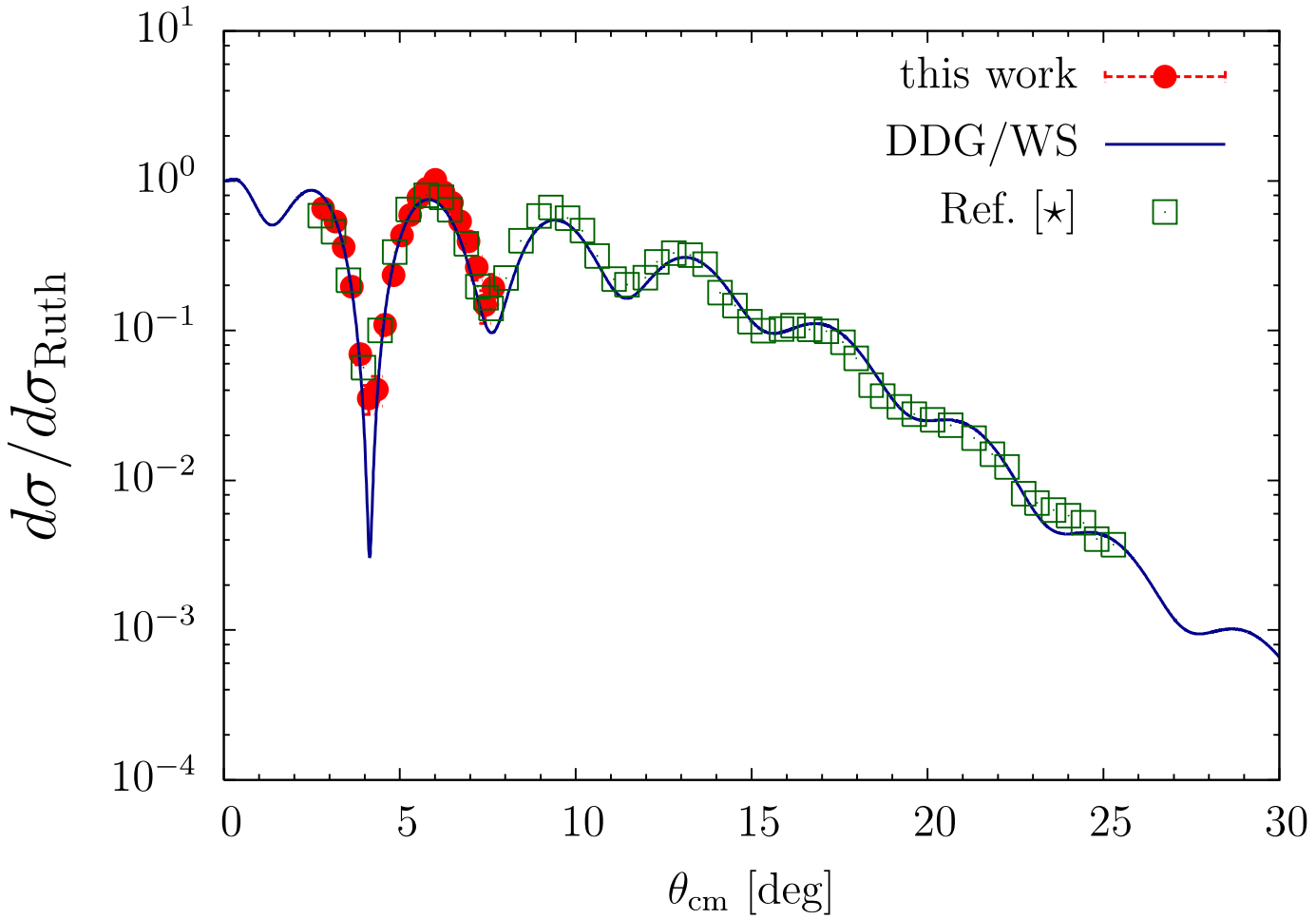

* B.K. Nayak *et al.*, Phys. Lett. *B* 637 (2006) 43

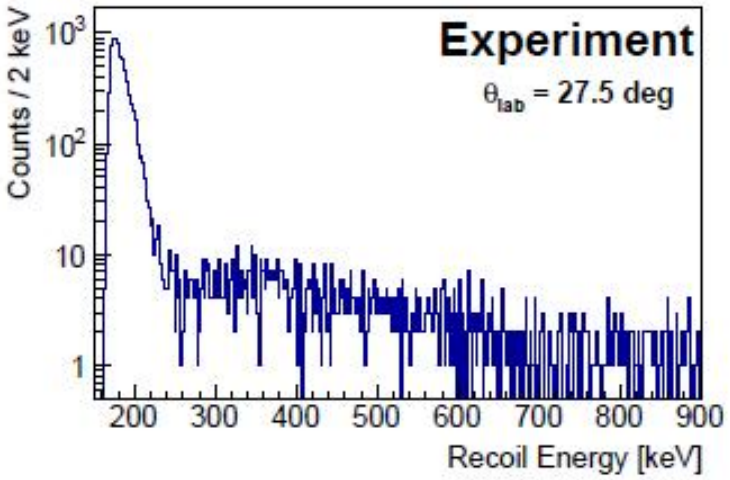

(a) Experiment, strip number 0

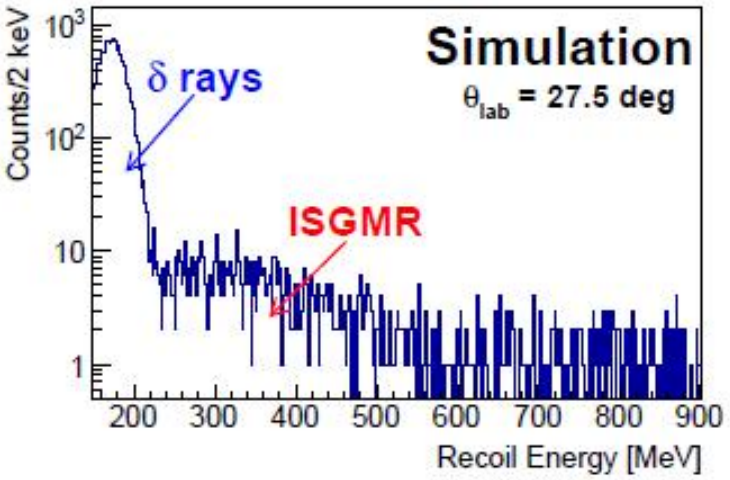

(b) Simulation, strip number 0.

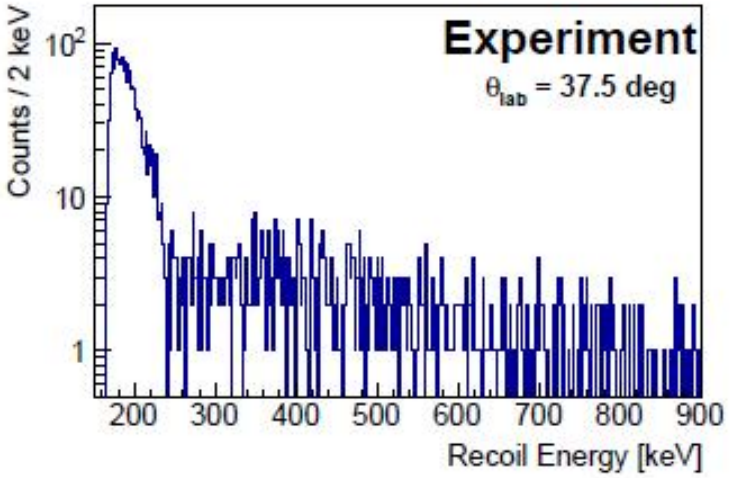

(c) Experiment, strip number 31

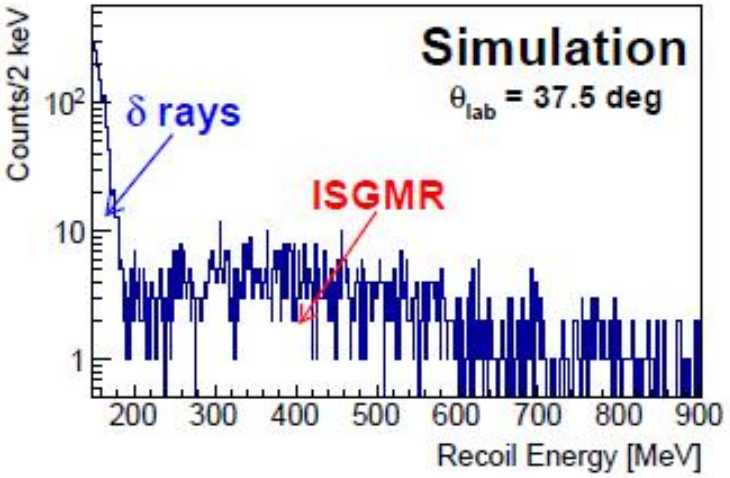

(d) Simulation, strip number 31

Inelastic alpha scattering (100 MeV/nucleon, PhD J.C. Zamora)

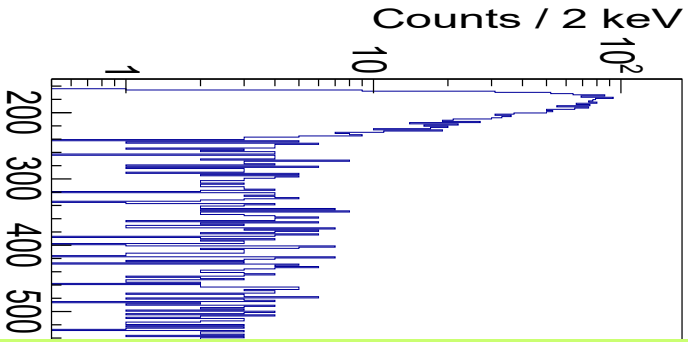

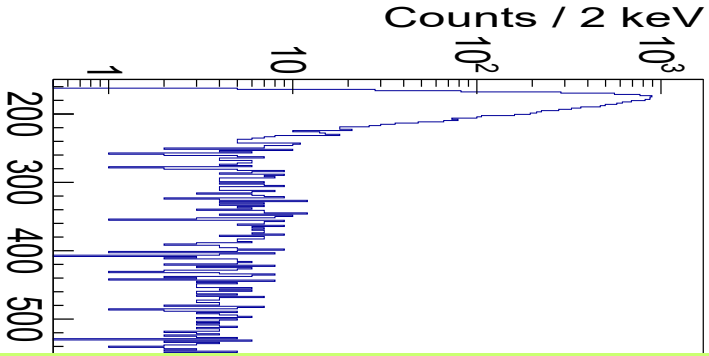

	Centroid [MeV]	$\text{Width}_{\text{rms}}$ [MeV]
this work	19(1)	5(1)
PRC **61**, 067307 (2000)	$20.3^{+1.7}_{-0.1}$	$4.3^{+0.7}_{-0.2}$
PRC **73**, 014314 (2006)	$19.2^{+0.4}_{-0.2}$	$4.9^{+1.1}_{-0.3}$
Phys. Lett. B **637**, 43 (2006)	$19.9^{+0.7}_{-0.8}$	–

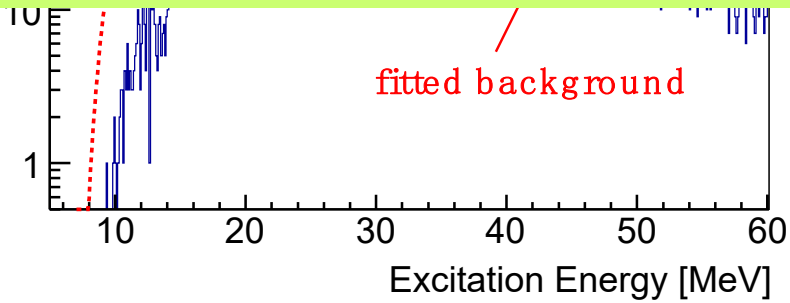

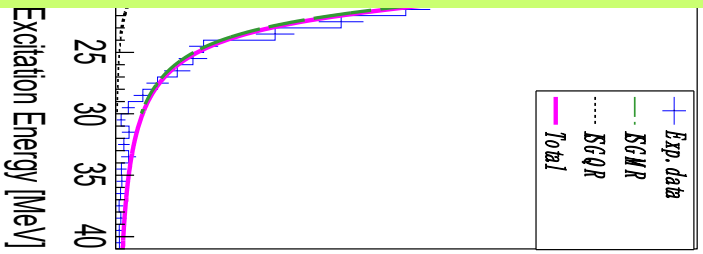

Inelastic alpha scattering (100 MeV/nucleon) from ^{58}Ni

J.C. Zamora, PhD work [J.C. Zamora *et al.*, Phys. Lett. B763 (2016) 16-19]

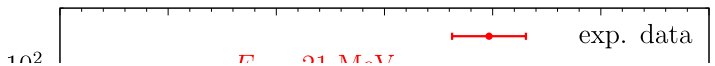

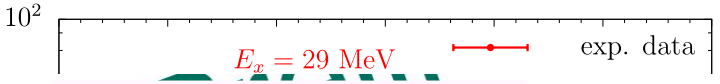

(centroid)

m_1/m_0 [MeV]	EWSR [%]	
21^{+5}_{-3}	86^{+17}_{-9}	this work
$20.3^{+1.7}_{-0.1}$	74^{+22}_{-12}	PRC **61**, 067307 (2000)
$19.9^{+0.7}_{-0.8}$	92^{+4}_{-3}	Phys. Lett. B **637**, 43 (2006)
20.8	108	RPA calculation *

* G. Colò et al, Comput. Phys. Commun. 184 (2013)

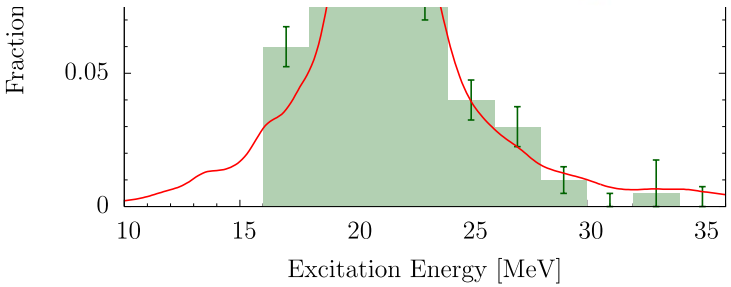

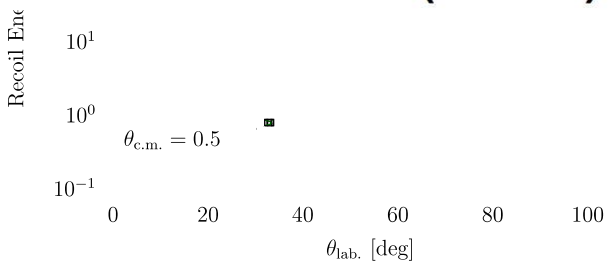

Monopole mode in ^{58}Ni and ^{56}Ni

Ring vs. Active target

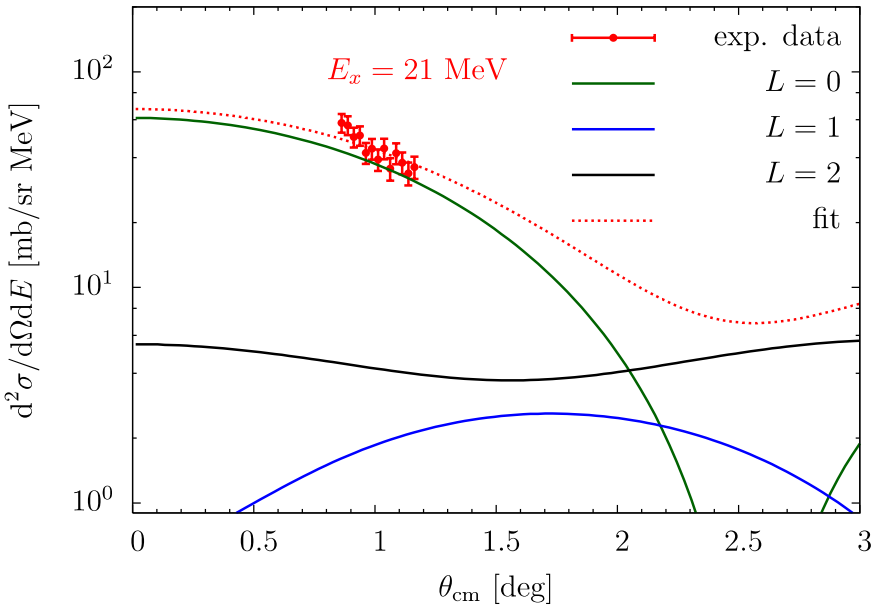

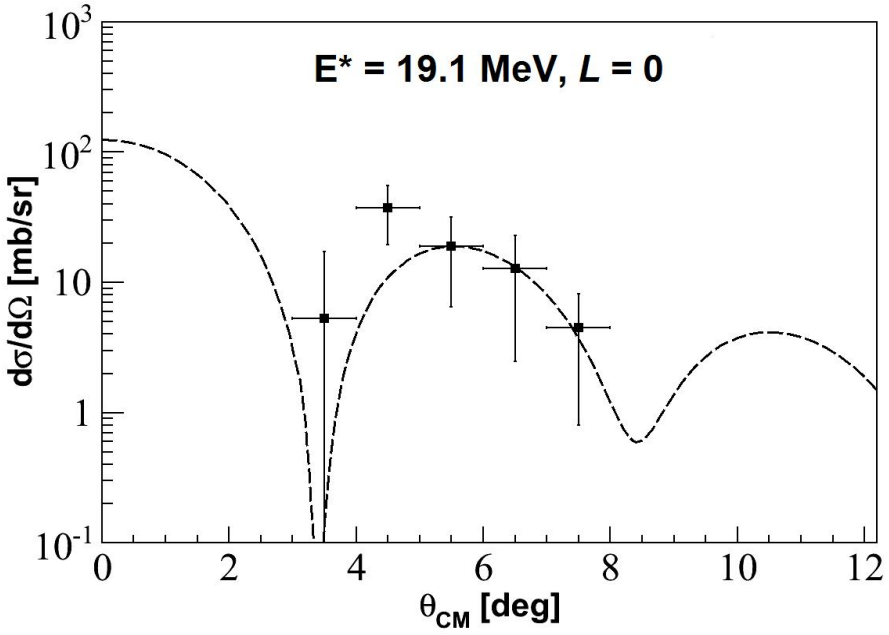

^{58}Ni

^{56}Ni

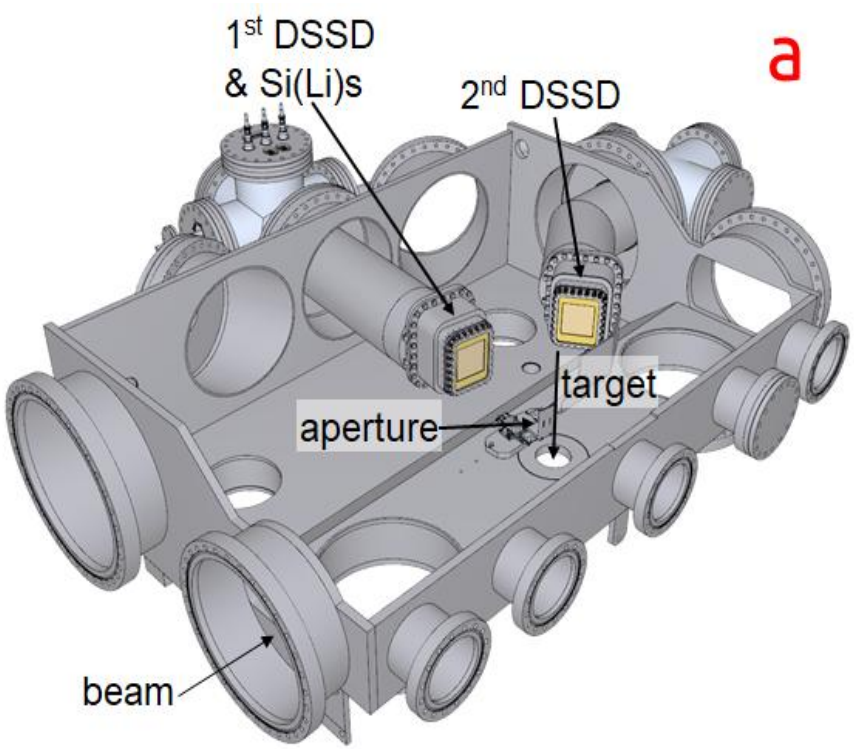

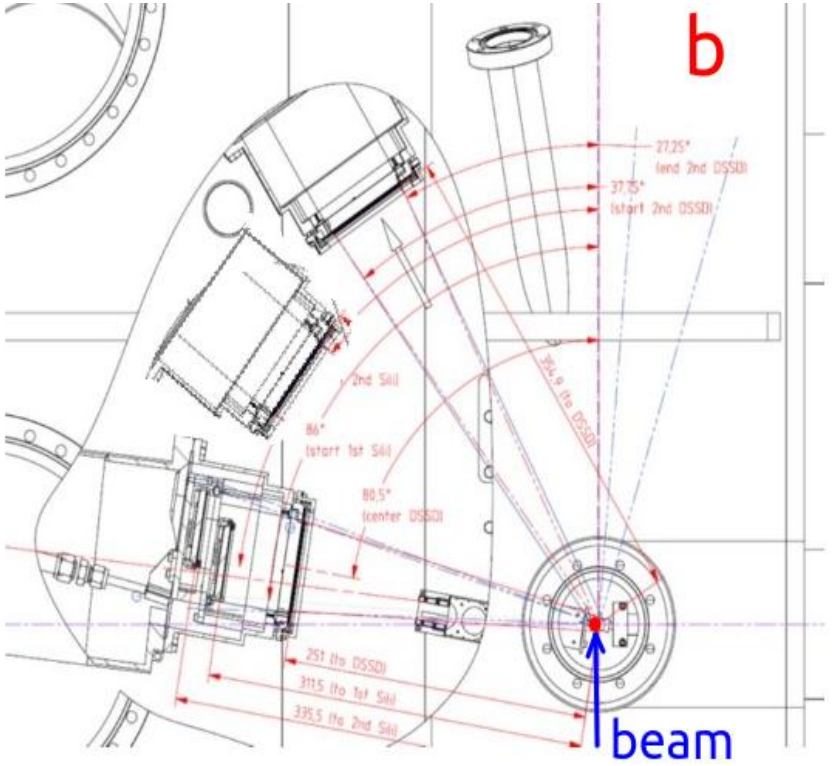

a) Drawing of the UHV-compatible scattering chamber The detectors were centred at 80° and 32° with respect to the beam direction.

b) Sketch of the upgraded experimental setup for the proposed experiment. A new detector will be installed in between the two existing pockets covering angles from 47° to 60°.

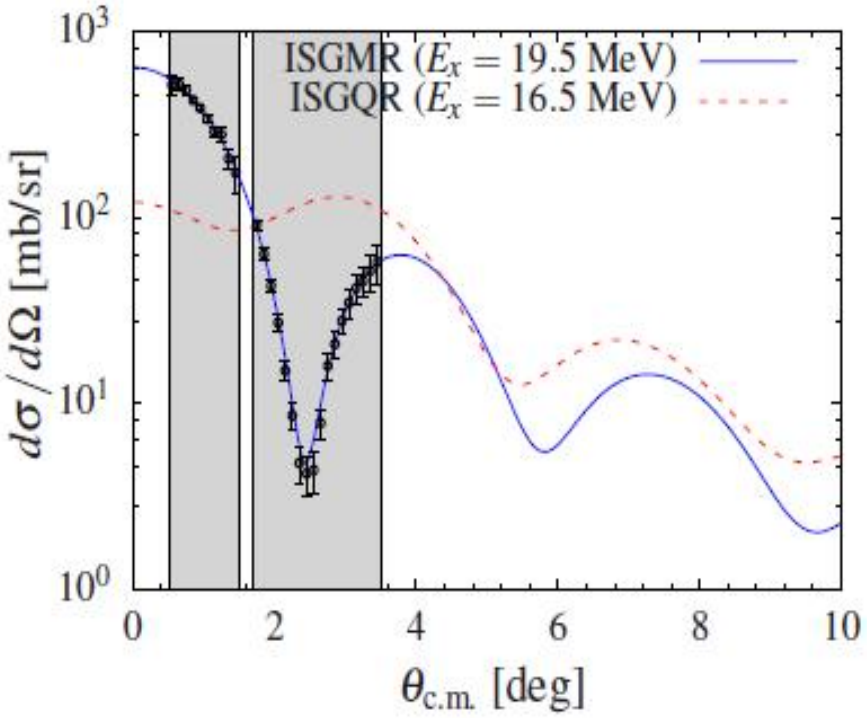

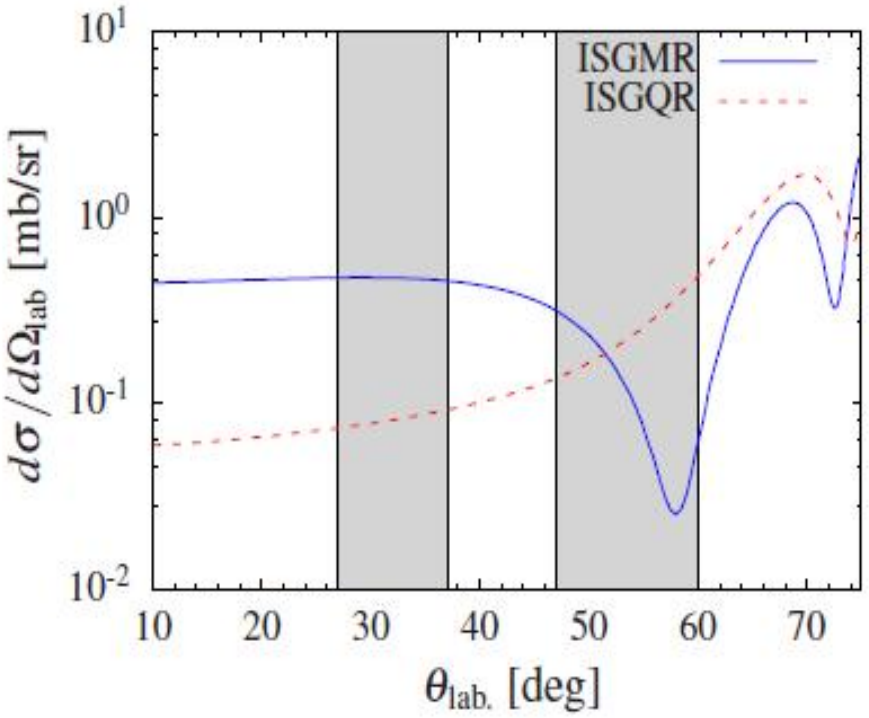

DWBA for the ISGMR and the ISGQR in ^{56}Ni at 100 MeV/u for inelastic scattering off ^{4}He assuming exhaustion of 100% of the respective EWSR.

Angular distributions in centre-of-mass frame (left) and in laboratory frame (right). The shadowed regions mark the angular range covered by the detector set-up in the proposed experiment. The data points (Monte-Carlo simulation) show the expected statistical uncertainty for the ISGMR with the requested beam time (14 days).

E605: ISGDR in ^{56}Ni

Linda Achouri
Hidetoshi Akimune
Soumya Bagchi
Konstanze Boretzky
Haïfa Bouzomita
Lucia Caceres
Franck Delaunay
Manuel Caamaño
Beatriz Fernandez
Mamoru Fujiwara
Umesh Garg
Julien Gibelin
Geoff Grinyer
Muhsin N. Harakeh
Nasser Kalantar-Nayestanaki
Omar Kamalou
Elias Khan
Attila Krasznahorkay
Gregoire Lhoutellier
Sergei Lukyanov
Katarzyna Mazurek
Mohammad Ali Najafi
Julien Pancin
Yuri Penionzkhevich
Luc Perrot
Riccardo Raabe
Catherine E. Rigollet
Thomas Roger
Sara Sambi
Hervé Savajols
Christelle Stodel
Laura Suen
Jean Charles Thomas
Marine Vandebrouck
Jarno van de Walle

The EXL-E105 Collaboration

S. Bagchi[1], S. Bönig[2], M. Castlós[3], I. Dillmann[4], C. Dimopoulou[4], P. Egelhof[4], V. Eremin[5], H. Geissel[4], R. Gernhäuser[6], M.N. Harakeh[1], A.-L. Hartig[2], S. Ilieva[2], N. Kalantar-Nayestanaki[1], O. Kiselev[4], H. Kollmus[4], C. Kozhuharov[4], A. Krasznahorkay[3], T. Kröll[2], M. Kuilman[1], S. Litvinov[4], Yu.A. Litvinov[4], M. Mahjour-Shafiei[1], M. Mutterer[4], D. Nagae[8], M.A. Najafi[1], C. Nociforo[4], F. Nolden[4], U. Popp[4], C. Rigollet[1], S. Roy[1], C. Scheidenberger[4], M. von Schmid[2], M. Steck[4], B. Streicher[2,4], L. Stuhl[3], M. Takechi[4], M. Thürauf[2], T. Uesaka[9], H. Weick[4], J.S. Winfield[4], D. Winters[4], P.J. Woods[10], T. Yamaguchi[11], K. Yue[4,7], J.C. Zamora[2], J. Zenihiro[9]

[1] ***KVI-CART, Groningen***
[2] ***Technische Universität Darmstadt***
[3] ***ATOMKI, Debrecen***
[4] ***GSI, Darmstadt***
[5] ***Ioffe Physico-Technical Institute, St. Petersburg***
[6] ***Technische Universität München***
[7] ***Institute of Modern Physics, Lanzhou***
[8] ***University of Tsukuba***
[9] ***RIKEN Nishina Centre***
[10] ***The University of Edinburgh***
[11] ***Saitama University***

Thank you for your attention

For the equation of state of symmetric nuclear matter at saturation nuclear density:

$$\left[\frac{d(E/A)}{d\rho}\right]_{\rho=\rho_0} = 0$$

and one can derive the incompressibility of nuclear matter:

$$K_{nm} = \left[9\rho^2 \frac{d^2(E/A)}{d\rho^2}\right]_{\rho=\rho_0}$$

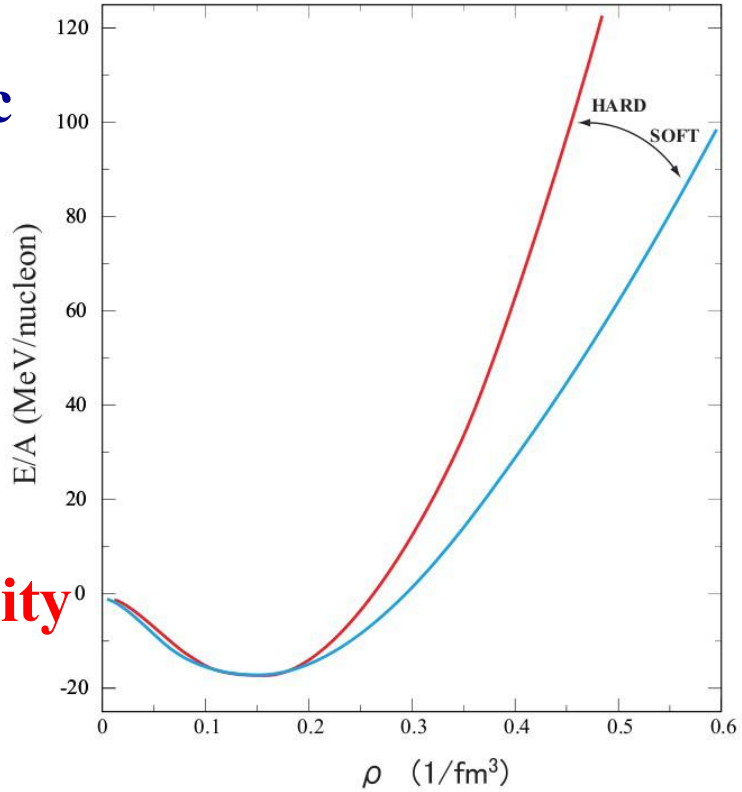

***E/A*: binding energy per nucleon**

ρ : nuclear density

ρ_0 : nuclear density at saturation

J.P. Blaizot, Phys. Rep. 64 (1980) 171

Beam subtraction

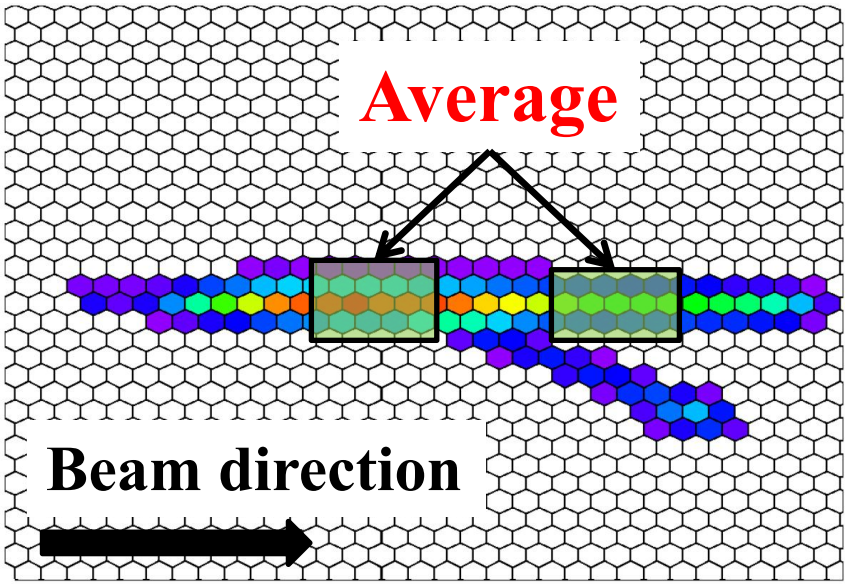

Extrapolated beam

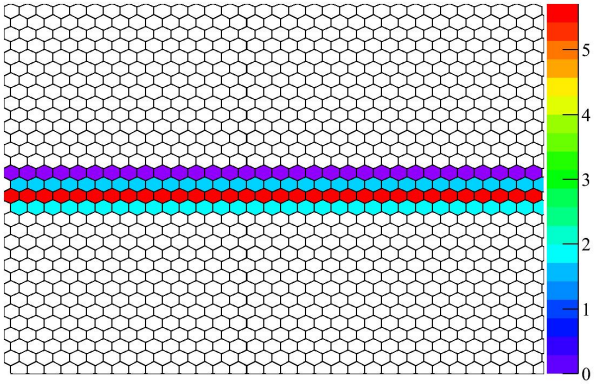

Beam subtracted

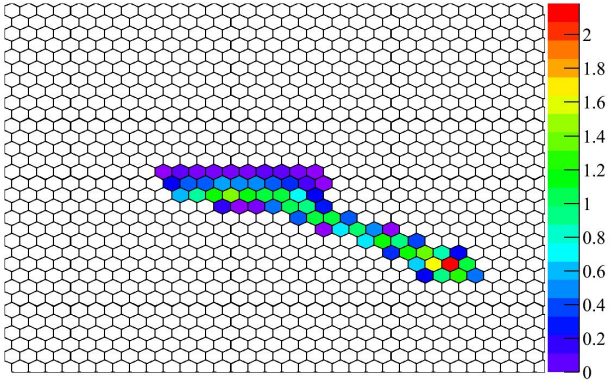

Long recoil track fitting

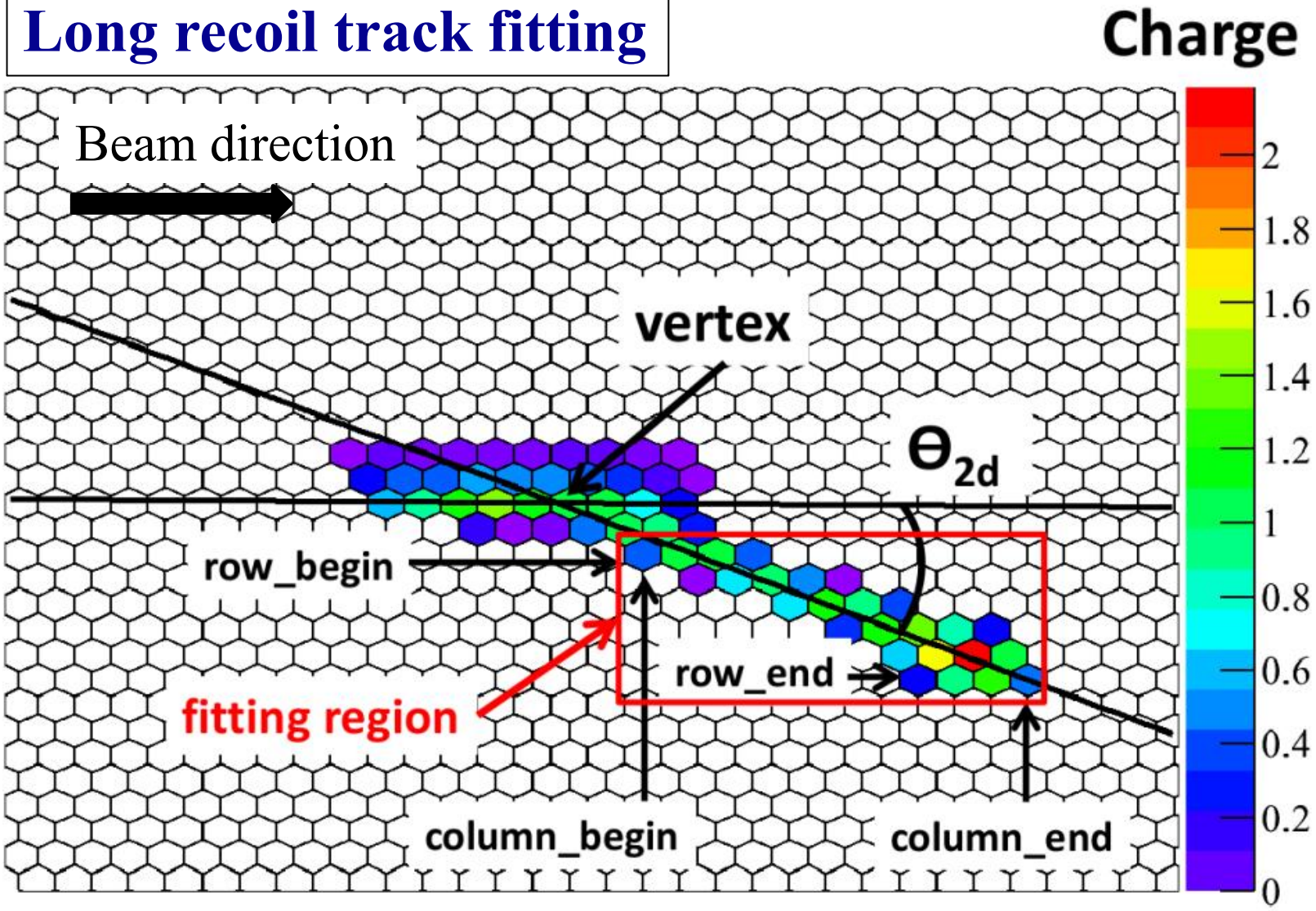

Short recoil track fitting